Molecular Therapy
Oncolytics
Original Article

lncRNA *RP11-147L13.8* suppresses metastasis and chemo-resistance by modulating the phosphorylation of c-Jun protein in GBC

Bohao Zheng,[1,2,3,4,5,7] Jiwen Wang,[1,2,3,4,5,7] Kun Fan,[1,2,3,4,5,6,7] Wentao Sun,[1,2,3,4,5] Wenze Wan,[1,2,3,4,5] Zhihui Gao,[2] Xiaojian Ni,[1,2,3,4,5] Dexiang Zhang,[5,6] Xiaoling Ni,[1,2,3,4,5] Tao Suo,[1,2,3,4,5] Han Liu,[1,2,3,4,5] Houbao Liu,[1,2,3,4,5,6] and Sheng Shen[1,2,3,4,5,6]

[1]Department of General Surgery, Zhongshan Hospital, Fudan University, 180 Fenglin Road, Shanghai 200032, China; [2]Biliary Tract Disease Center of Zhongshan Hospital, Fudan University, Shanghai 200032, China; [3]Cancer Center, Zhongshan Hospital, Fudan University, Shanghai 200032, China; [4]Biliary Tract Disease Institute, Fudan University, Shanghai 200032, China; [5]Shanghai Biliary Tract Minimal Invasive Surgery and Materials Engineering Research Center, Shanghai 200032, China; [6]Department of General Surgery, Shanghai Xuhui Central Hospital, Zhongshan-Xuhui Hospital, Fudan University, Shanghai 200032, China

Long non-coding RNAs (lncRNAs) have been identified as critical contributors in tumor progression for many types of cancer. However, their functions in gallbladder cancer (GBC) have not been systematically clarified. In this study, the clinical significance, biological function, and underlying mechanism of lncRNA *RP11-147L13.8* in GBC were investigated. The quantitative real-time PCR result indicated that lncRNA *RP11-147L13.8* was found to be recurrently downregulated in GBC tumor samples. Kaplan-Meier analysis revealed that decreased lncRNA *RP11-147L13.8* expression level was associated with poor survival of GBC patients (p = 0.025). Then, both *in vitro* and *in vivo* experiments elucidated that the overexpression of lncRNA *RP11-147L13.8* suppressed the migration and invasion abilities of GBC cells and promoted the sensitivity to gemcitabine of GBC cells. Furthermore, we found that lncRNA *RP11-147L13.8* physically interacted with c-Jun protein and decreased the phosphorylation on serine-73 (c-Jun-Ser73), which might cause the enhancement of the migration, invasion, and sensitivity to gemcitabine of GBC tumor cells. In conclusion, our study identified lncRNA *RP11-147L13.8* as a promising prognostic indicator for patients with GBC, providing insights into the molecular pathogenesis of GBC. lncRNA *RP11-147L13.8* is a potential therapeutic combination for gemcitabine in GBC treatment.

INTRODUCTION

Gallbladder cancer (GBC), the most common biliary tract malignancy, is also the fifth most common digestive tract malignancy worldwide, with approximately 2.5 in 100,000 persons affected.[1,2] The prognosis of advanced GBC is poor, with a survival time of less than 1 year, regardless of adjuvant therapy of standard chemotherapy.[3] Currently, surgical resection remains the only curative treatment for GBC patients, with a 5-year survival rate of 90% for T1-stage patients.[4] However, due to the lack of specific symptoms and signs, the majority of GBC patients were diagnosed at an advanced stage and not appropriate for resection. Herein, the prognosis of gallbladder cancer is dismal. The emergence of adjuvant therapy based on chemotherapy provided a chance to prolong the survival of patients with gallbladder cancer.[5] Unfortunately, it has been reported that GBC is not sensitive to chemotherapeutic drugs.[6] Hence, it is urgent to reveal the underlying molecular mechanisms associated with GBC chemo-resistance and figure out the way to solve it.

With the wide application of next-generation sequencing, more and more long non-coding RNAs (lncRNAs) have been identified. lncRNAs are defined as transcripts composed of more than 200 bp in length with no or weak protein-coding abilities, which was previously recognized as transcriptional "noise" initially.[7] In recent years, many functions of lncRNAs have been reported in regulating various biological processes, such as cell differentiation, apoptosis, and immune escape.[8] Besides, lncRNAs could exert their biological function by preventing RNA and protein from binding to intended targets, acting as host genes for microRNAs, and serving as molecular scaffolds to guide proteins to their direct chromosomal targets.[9–11] Recently, accumulating evidence indicated that lncRNAs contribute a lot to the initiation and progression of the tumor, including hepatocellular carcinoma, colorectal carcinoma, and cholangiocarcinoma.[12–14] As for GBC, increasing attention has been attracted by the biological

Received 9 March 2021; accepted 31 August 2021;
https://doi.org/10.1016/j.omto.2021.08.016.

[7]These authors contributed equally

Correspondence: Han Liu, MD, PhD, Department of General Surgery, Zhongshan Hospital, Fudan University, 180 Fenglin Road, Shanghai 200032, China.
E-mail: liu.han@zs-hospital.sh.cn
Correspondence: Houbao Liu, MD, PhD, Department of General Surgery, Zhongshan Hospital, Fudan University, 180 Fenglin Road, Shanghai 200032, China.
E-mail: liu.houbao@zs-hospital.sh.cn
Correspondence: Sheng Shen, MD, PhD, Department of General Surgery, Zhongshan Hospital, Fudan University, 180 Fenglin Road, Shanghai 200032, China.
E-mail: shen.sheng@zs-hospital.sh.cn

role of lncRNA in cancer progression. For instance, a lncRNA *PVT1* has been reported in the tumor progression of GBC through regulating the miR-143/hexokinase 2 (HK2) axis in GBC.[15] Another lncRNA *H19* was also reported that could influence the progression of GBC through regulating *FOXM1* expression by competitively binding endogenous *miR-342-3p*.[16] Moreover, lncRNA *GBCDRlnc1* could regulate the autophagy process to promote the chemo-resistance of the gallbladder.[17]

Oncogene *c-Jun* is located in the 1p32.1 region of the human chromosome, and its encoded protein was identified as FOS binding protein P39, which was composed of 334 amino acids.[18] c-Jun protein has two major separate protein domains that could be phosphorylated. One is located at the C-terminal, which is very close in proximity to the DNA binding domain. These sites are Thr214, Ser226, and Ser 232, which are often phosphorylated by glycogen synthase kinase 3 (GSK3) and casein kinase (CK2II) phosphorylases. When these sites are dephosphorylated, c-Jun protein will be released from the inhibitory effect of cell resting-state factor to promote the cell growth. Another phosphorylation domain has a high affinity in the ser63, ser73, c-Jun NH2-terminal kinases (JNKs), and delta domains in the transactivated domain. The phosphorylation of ser63 and ser73 would rapidly induce the transcriptional activation function.[19] The function of the c-Jun DNA binding and dimerization domain is to bind DNA and form a basic leucine zipper domain with the FOS family or other jun family proteins. This homologous or dimerization binding constitutes an important transcription factor activating protein 1 (AP-1), which plays a role in transcriptional activation. Specifically, several studies have shown that phosphorylation of ser63 and ser73 sites of c-*jun* can affect cell growth, differentiation, apoptosis, and other biological functions through the JNK signaling pathway and promote the occurrence and development of human malignant tumors.[20,21] Recent studies have found the aberrant expression of c-Jun exists in gallbladder carcinoma, which may be closely related to the occurrence and development of gallbladder carcinoma. Additionally, many studies have found that c-Jun, a key gene of the JNK signaling pathway, plays a key role in regulating chemotherapy resistance in human malignant tumors. For instance, Roszak et al.[22] found that c-Jun was upregulated in leukemia cells HL-60 and promoted arsenic trioxide drug resistance by regulating the JNK signaling pathway. However, it remains unclear how the c-*jun* influences chemo-resistance in GBC, which deserves further exploration.

In our study, we characterized the transcriptional landscape of lncRNAs in paired GBC tissues and drug-resistant GBC cell lines and identified hundreds of lncRNAs that showed dysregulation in GBC tumor samples. We found and further validated that the long intergenic non-coding RNA, lncRNA *RP11-147L13.8*, was recurrently downregulated in GBC tumor tissue and drug-resistant cell lines. Moreover, its low expression predicted poor outcomes for GBC patients. Functional assays in GBC cell lines revealed that lncRNA *RP11-147L13.8* could substantially suppress the migration and invasion of GBC tumor cells both *in vitro* and *in vivo*. Besides, our study suggested that the overexpression of lncRNA *RP11-147L13.8* could enhance gemcitabine sensitivity on GBC cells. In terms of the underlying mechanism, our further analysis revealed that lncRNA *RP11-147L13.8* physically interacted with c-Jun protein by binding delta bZIP domain to inhibit the phosphorylation of c-*jun*-Ser73 in GBC cell lines. Our study shed light on the molecular mechanisms underlying the progression of GBC and provided insights into the therapeutic strategy for GBC patients.

RESULTS

Transcriptional landscape and dysregulation of lncRNAs in GBC

The expression profiles of four paired GBC samples were extracted to investigate the comprehensive dysregulation and potential biological roles of lncRNAs in the carcinogenesis processes of GBC. Our analysis detected 1,012 lncRNAs and 1,254 mRNAs that showed different expression levels in the microarray data (Figure 1A). Then, the further Gene Ontology (GO) analysis indicated that these different expressed lncRNAs and mRNAs might be involved in five biological processes, including transmembrane transport, cell-cell signaling, Jun-mitogen-activated protein kinase (MAPK) signaling pathway, transmembrane receptor protein tyrosine kinase signaling pathway, and cation transport (Figure 1B). Furthermore, to investigate the potential biological role of lncRNA in the drug resistance in GBC, the expression profiles of normal GBC-SD and drug-resistant GBC-SD cell lines were obtained and analyzed, which turned out that 1,092 lncRNAs showed different expression level (Figure 1C). We found out that 211 lncRNAs were both differentially expressed in GBC tumor tissue and drug-resistant GBC cell lines (Figures 1D and 1E). Besides, the top ten upregulated and downregulated differently expressed lncRNAs (Figures S1A and S1B) were validated in 24 pairs of GBC and adjacent normal tissues, which turned out that only RP11-147L13.8 WAS significantly downregulated in tumor tissues (Figure S1C). Finally, the expression level of this lncRNA was lower in drug-resistant tumors and drug-resistant GBC-SD cell lines (Figure 1F). Therefore, we hypothesized that lncRNA *RP11-147L13.8* might be related to the tumor formation and chemo-resistance in GBC, and further investigation was conducted.

RP11-147L13.8 is recurrently downregulated and associated with poor overall survival outcomes in GBC patients

To investigate the clinical significance of *RP11-147L13.8*, qPCR was used to evaluate the expression of this lncRNA in 96 paired GBC patients, which turned out that this lncRNA was significantly downregulated in GBC tumor tissues, as compared with the adjacent no-tumor tissues ($p < 0.0001$; Figure 2A). Detail clinicopathological parameters have been listed in Table 1. Further analyses indicated that the expression level of *RP11-147L13.8* was significantly lower in patients with venous invasion as compared with patients without venous invasion ($p = 0.0115$; Figure 2B). In the meantime, the expression level of this lncRNA was significantly lower in patients with advanced tumor, lymph node, metastasis (TNM) stage (Figure 2C). Then, the median expression level was selected as the cutoff value for this lncRNA. Accordingly, patients were divided into high and low groups. Survival analysis indicated that patients in the low group were associated with poor 5-year overall survival ($p = 0.025$; Figure 2D). Besides, high

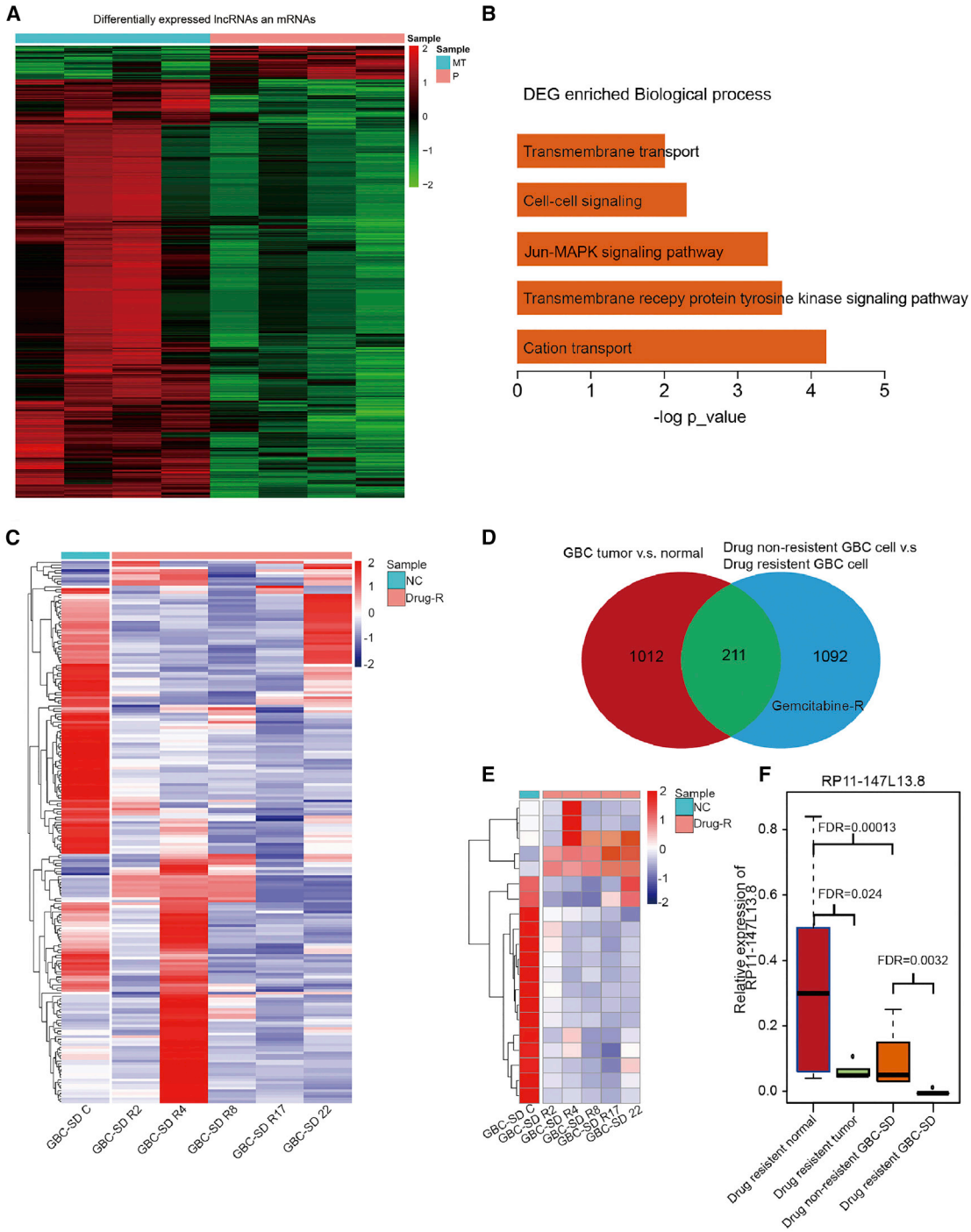

Figure 1. The expression level of long non-coding RNA *RP11-147L13.8* was downregulated in tumor tissue and chemo-resistant cell lines in gallbladder cancer

(A) The heatmap presented the expression level of the expression profiles of lncRNAs and mRNAs between 4 pairs of GBC tissue and normal tissue. (B) The differentially expressed genes (DEGs) enriched biological process includes transmembrane transport, cell-cell signaling, Jun-MAPK signaling pathway, transmembrane receptor protein tyrosine kinase signaling pathway, and cation transport. (C) The DEGs between GBC-SD and drug-resistant GBC-SD cells are shown. (D) 1,223 genes were differently expressed between GBC tumor tissues and normal tissues, although 1,303 genes were differentially expressed between normal GBC cell lines and drug-resistant GBC cell lines. Besides, 211 overlap genes were found between two gene sets. (E) The top 20 different expressed lncRNAs between GBC-SD and drug-resistant GBC-SD cell lines are shown. (F) The expression level of RP11-147L13.8 was significantly downregulated in drug-resistant tumor tissues and drug-resistant GBC-SD cell lines.

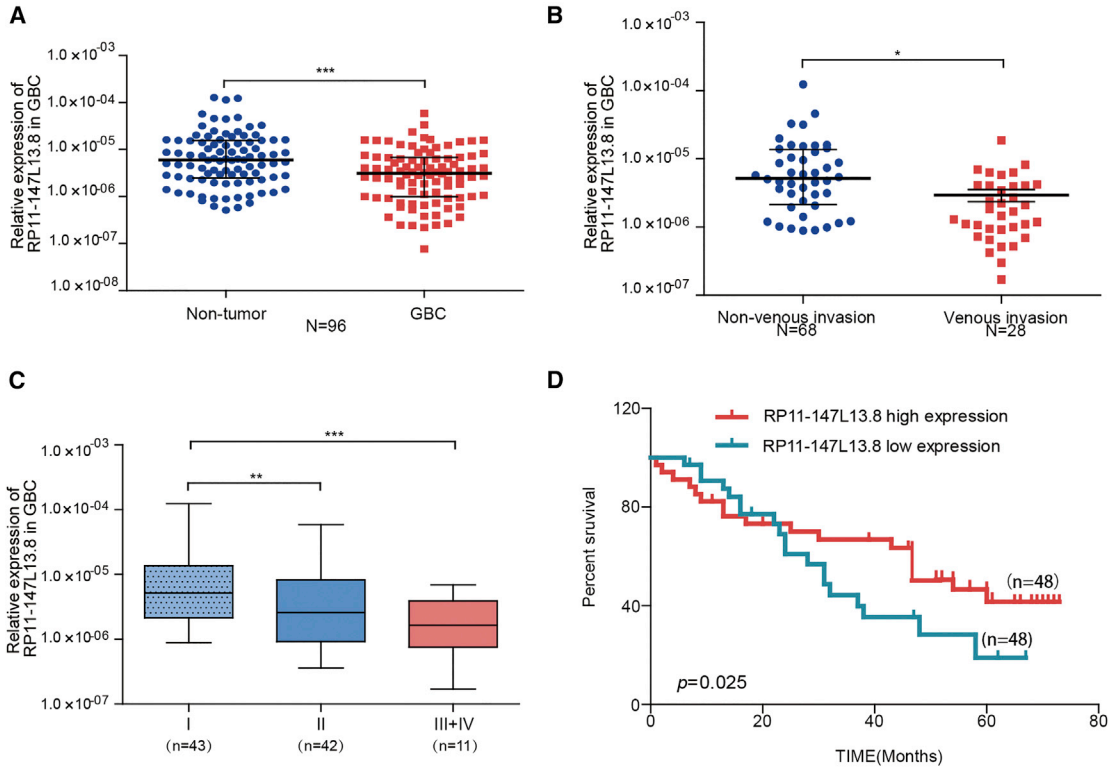

Figure 2. The clinical and prognostic significances of *RP11-147L13.8* in GBC patients

(A) *RP11-147L13.8* is downregulated in tumor tissue compared with the adjacent non-tumor tissue (n = 96). Data represent median ± 95% confidence interval (CI). Wilcoxon signed rank test. *p < 0.05; **p < 0.001; ***p < 0.0001. (B) *RP11-147L13.8* is downregulated in tumor tissue with venous invasion compared with the adjacent non-tumor tissue. Data represent median ± 95% confidence interval (CI). Wilcoxon signed-rank test. *p < 0.05; **p < 0.001; ***p < 0.0001. (C) The expression level of *RP11-147L13.8* is lower in GBC patients with advanced TNM stage. Data represent median ± 95% confidence interval (CI). Wilcoxon signed-rank test. *p < 0.05; **p < 0.001; ***p < 0.0001. (D) Patients with low expression of *RP11-147L13.8* were associated with poorer overall survival (log rank test; p = 0.025).

expression level of this lncRNA positively correlated with small tumor size, lower venous invasion rate, and early TNM stage in GBC patients (Table 2). Therefore, these results indicated that *RP11-147L13.8* was a potential prognostic biomarker for GBC patients and might be involved in the formation and metastasis of GBC.

The detailed information of this lncRNA was presented in Figures S2 and S3. The lncRNA *RP11-147L13.8* was predicted to possess no protein-coding potential by the LNCipedia database (Figure S2).[23] Meanwhile, Coding-Potential Assessment Tool (CPAT) online software[24] could not predict the protein-coding potentiality of this lncRNA (Figure S2). The expression profile of this lncRNA across pan-human cancer and pan-human tissues was presented in Figure S3A. The 5′ and 3′ rapid amplification of complementary DNA ends (RACE) assays revealed the full length of RP11-147L13.8 dominant isoform is about 2,919 bp (Figure S3B). The expression levels of *RP11-147L13.8* were different across different GBC cell lines, wherein GBC-SD cells expressed the highest *RP11-147L13.8* and NOZ expressed the lowest (Figure S3C). Besides, *RP11-147L13.8* was expressed in both cytoplasm and nucleus (cytoplasm: 35%; nucleus: 65%; Figure S3D).

RP11-147L13.8 suppresses migration and invasion abilities of GBC cells *in vitro* and *in vivo*

To investigate the biological function of RP11-147L13.8, a stable knockdown and overexpression cell line was constructed; the altered change in the expression level of this lncRNA was presented in Figure S3E. Next, functional assays were further performed to determine the biological effects of *RP11-147L13.8* on GBC cell lines. The knockdown of *RP11-147L13.8* significantly promoted the migration and invasion abilities of GBC-SD cell lines, although the overexpression of *RP11-147L13.8* significantly suppressed the migratory and invasive abilities of GBC-SD cell lines (Figures 3A and 3B). Similar results were observed in NOZ cell lines (Figures 3C and 3D). These results suggested that *RP11-147L13.8* could suppress the migratory and invasive abilities of GBC tumor cells *in vitro*.

In vivo experiment was further carried out to demonstrate the effects of *RP11-147L13.8* on cell migration and metastasis. No significant differences were observed in the tumor volume and tumor weight. The metastatic nodules in both liver and lung were significantly increased in the *RP11-147L13.8* knockdown group. Furthermore,

Table 1. The baseline information of the 96 GBC patients enrolled in this study

Characteristics	Patient number
Age, years	
≤60 years	50
>60 years	46
Gender	
Male	56
Female	40
Diabetes mellitus	
No	53
Yes	43
CA19-9[a] (U/mL)	
≤37	47
>37	43
Tumor size (cm)	
≤2.5	56
>2.5	40
Lymph node metastasis	
No	54
Yes	42
Grade	
Well-differentiated	21
Moderately differentiated	46
Poorly differentiated	29
TNM stage	
I	43
II	42
III+IV	11

[a]CA19-9 data are from 90 patients (data missing for 6 patients).

Table 2. Correlations between the *RP11-147l13.8* expression level and clinicopathological characteristics in GBC patients

	RP11-147l13.8		
Characteristics	Low (n = 48)	High (n = 48)	p value
Age, years			
≤60	27	23	0.414
>60	21	25	
Gender			
Female	29	27	0.679
Male	19	21	
Diabetes mellitus			
No	25	28	0.538
Yes	23	20	
CA 19-9 (U/mL)			
≤37	26	21	0.841
>37	19	24	
Tumor size (cm)			
≤2.5	21	35	0.004
>2.5	27	13	
Venous invasion			
No	28	40	p < 0.001
Yes	20	8	
Grade			
Well-differentiated	7	14	0.224
Moderately differentiated	25	21	
Poorly differentiated	16	13	
TNM stage			
I+II	39	46	0.025
III+IV	9	2	

Pearson chi-square test and Fisher's exact test. CA 19-9, carbohydrate antigen 19-9; TNM, tumor, lymph node, metastasis.

the hematoxylin and eosin (H&E) staining results showed a dramatic increase of metastatic foci derived from cells of the *RP11-147L13.8* knockdown group in liver and lung tissue sites (Figures S4E and S4F). Thus, these observations demonstrated that *RP11-147L13.8* might suppress the tumor metastasis both *in vitro* and *in vivo*.

RP11-147L13.8 enhances drug sensitivity of gemcitabine in GBC tumor cell lines

To further explore the functional role of *RP11-147L13.8* in the drug resistance of GBC, we investigated its effects on the treatment with gemcitabine, which is usually used in chemotherapy for GBC patients. The knockdown of *RP11-147L13.8* dramatically increased the IC_{50} in gemcitabine-treated GBC-SD cells (short hairpin RNA for RP11-147L13.8 (shNC) versus shlnc(mix):5.7 μg/mL versus 23.07 μg/mL; Figure 3E). Moreover, the overexpression of *RP11-147L13.8* significantly reduces the IC_{50} in gemcitabine-treated NOZ cell lines (shNC versus shlnc(mix):4.46 μg/mL versus 12.61 μg/mL; Figure 3F).

RP11-147L13.8 interacts with c-Jun and suppresses the c-Jun-ser73 phosphorylation via inhibiting the JNK in GBC cells

For a better understanding of how *RP11-147L13.8* performs its activities in gallbladder carcinogenesis and tumor progression, RNA pull-down assays were conducted to identify *RP11-147L13.8*-related proteins in GBC cells. The mass spectrometry analyses following *RP11-147L13.8* pull-down experiments revealed specific protein bands that bind with the *RP11-147L13.8* (Figure 4A). Based on the filtrations of high-confidence scores (no less than 100 in mass spectrometric assays) and absence in corresponding anti-sense groups, nine proteins that might interact with *RP11-147L13.8* were obtained (Table S3). The *RP11-147L13.8*-c-Jun interaction was further verified by RNA immunoprecipitation (RIP) assays, wherein *RP11-147L13.8* was significantly enriched in c-Jun antibody, but not immunoglobulin G (IgG) control (Figure 4B). Our western blot results confirmed that c-Jun protein was specifically associated with sense, but not anti-sense,

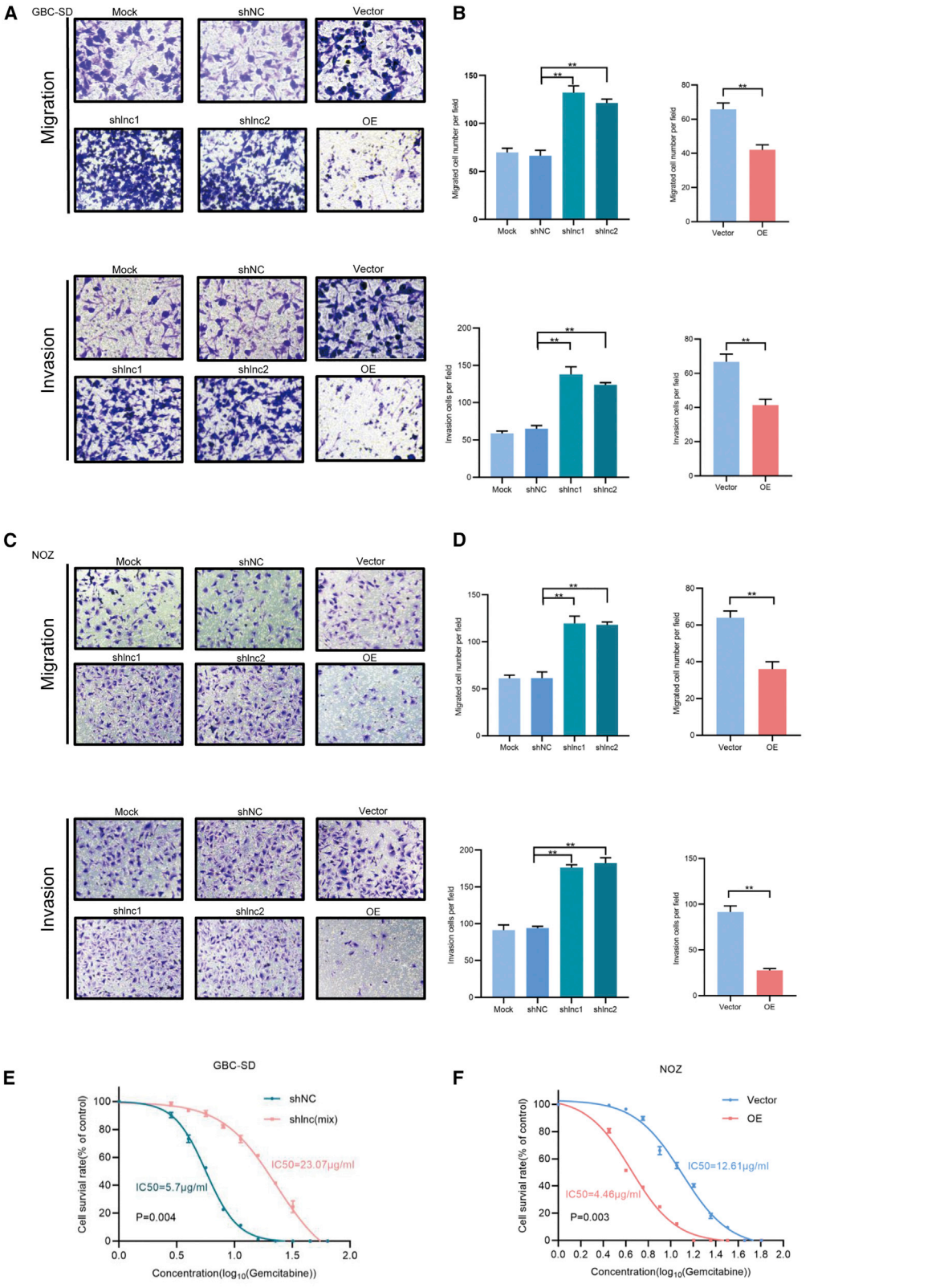

(legend on next page)

RP11-147L13.8 (Figure 4C). Besides, the western blot result indicated that the overexpression of *RP11-147l13.8* could suppress the ser73 phosphorylation of the c-Jun protein, although the knockdown of *RP11-147l13.8* could promote the ser73 phosphorylation of the c-Jun protein in both GBC-SD and NOZ cell lines (Figures 4D and 4E).

To further investigate how the lncRNA *RP11-147L13.8* influences the ser73 phosphorylation of the c-Jun protein, a co-immunoprecipitation (coIP) experiment was performed in the *RP11-147L13.8* knockdown and *RP11-147L13.8* overexpression GBC cell lines. The coIP results indicated that the overexpression of *RP11-147L13.8* could competitively inhibit the interaction between the JNK and c-Jun protein in both GBC-SD and NOZ, which results in the ser73 dephosphorylation of c-Jun protein (Figure 4F). In contrast, the knockdown of the *RP11-147L13.8* could promote the ser73 phosphorylation of c-Jun protein in two GBC cell lines (Figure 4G). Besides, the expression levels of c-Jun-ser73 in 24 GBC tissues were evaluated through immunohistochemistry (IHC) (Figure S5A). Then, Kaplan-Meier analysis indicated that patients with higher expression of c-Jun-ser73 phosphorylation were associated with poorer overall survival (Figure S5B). Meanwhile, our data indicated that the expression level of RP11-147L13.8 was negatively correlated with the expression level of c-Jun-ser73 ($R = -0.63$; $p = 0.002$; Figure S5C). Taken together, all these data indicated that RP11-147L13.8 could suppress the c-Jun-ser73 phosphorylation.

RP11-147L13.8 interacts with c-Jun via binding with the basic region leucine zipper (bZIP) Jun domain of the JUN protein

Further investigation was carried out to determine the biological roles of the specific *RP11-147L13.8* fragment that binds the c-Jun protein; a series of deletions was constructed to map the truncated *RP11-147L13.8* fragments with c-Jun protein. The results of deletion mapping analyses showed that the 2,215- to 2,919-nt fragment of *RP11-147L13.8* was required for its interaction with the c-Jun protein (Figures 5A and 5B). Moreover, our RIP assays revealed that the bZIP domain of c-Jun was responsible for the binding with *RP11-147L13.8* (Figure 5C). Specifically, the interaction between c-Jun and *RP11-147L13.8* was significantly abolished under the deletion of the bZIP_Jun domain (Figure 5D). In summary, all these data further demonstrated that *RP11-147L13.8* interacts with c-Jun via binding with the bZIP domain of the c-Jun protein, which might explain the biological function of this lncRNA.

The rescue assay confirmed that lncRNA RP11-147L13.8 performs its biological function by suppressing the c-Jun-ser73 phosphorylation in GBC cell lines

To further validate that RP11-147L13.8 performs its biological function through suppressing the c-Jun-ser73 phosphorylation, a rescue assay was performed. To reverse the c-Jun-ser73 phosphorylation, a point mutation experiment was carried out, which changed the Ser at 73 sites into Ala (Figure 6A). After transfection, the western blot result validated the efficiency of point mutation, which indicated that the point mutation could significantly inhibit the c-Jun-Ser 73 phosphorylation in both GBC-SD and NOZ cell lines (Figure 6B). Then, transwell assay indicated that the knockdown of this lncRNA could promote the migration (Figure 6C) and invasive (Figure 6D) ability of the GBC-SD cell line, although after the point mutation, the overexpression of this lncRNA could suppress the migration (Figure 6C) and invasive (Figure 6D) ability of GBC-SD. Meanwhile, similar results were observed in the NOZ cell line (Figures 6E and 6F). In terms of the influence on the drug-resistant ability of GBC cell lines, Cell Counting Kit-8 (CCK-8) assay indicated that the knockdown of this lncRNA could increase the IC_{50} value for gemcitabine in both GBC-SD (Figure 6G) and NOZ (Figure 6H) cell lines, indicating that knockdown of this lncRNA could promote the resistant ability to gemcitabine in both GBC-SD and NOZ cell lines. After the point mutation, the IC_{50} value for gemcitabine significantly decreased in both GBC-SD (Figure 6G) and NOZ (Figure 6H) cell lines, indicating that point mutation could reverse the biological effect of this lncRNA on the gemcitabine-resistant ability of GBC cell lines.

Taken together, all these results confirmed that lncRNA RP11-147L13.8 performs its biological function by suppressing the c-Jun-ser73 phosphorylation in GBC cell lines.

DISCUSSION

Recently, many findings suggest that lncRNAs play an important role in the initiation and progression of GBC. Here, we investigated the clinical significance and biological role of a novel lncRNA *RP11-147L13.8* in GBC. In terms of the clinical significance, the lower expression of this lncRNA was associated with a higher lymph

Figure 3. The overexpression of lncRNA *RP11-147L13.8* suppressed the migration and invasion ability and enhanced the drug sensitivity in GBC cell lines

(A) The overexpression of lncRNA *RP11-147L13.8* suppressed the migration ability in GBC-SD cell lines, although the overexpression of lncRNA *RP11-147L13.8* suppressed the invasion ability in GBC-SD cell lines. Magnification, 200×. Data represent mean ± SEM (three biological replicates). Paired Student's t test. *$p < 0.05$; **$p < 0.001$; ***$p < 0.0001$. (B) The downregulation of lncRNA *RP11-147L13.8* promotes the migration ability in GBC-SD cell lines, although the downregulation of lncRNA *RP11-147L13.8* promotes the invasion ability in GBC-SD cell lines. Magnification, 200×. Data represent mean ± SEM (three biological replicates). Paired Student's t test. *$p < 0.05$; **$p < 0.001$; ***$p < 0.0001$. (C) The overexpression of lncRNA *RP11-147L13.8* suppresses the migration ability in NOZ cell lines, although the downregulation of lncRNA *RP11-147L13.8* promotes the migration ability in NOZ cell lines. Magnification, 200×. Data represent mean ± SEM (three biological replicates). Paired Student's t test. *$p < 0.05$; **$p < 0.001$; ***$p < 0.0001$. (D) The overexpression of lncRNA *RP11-147L13.8* suppresses the invasion ability in NOZ cell lines, although the downregulation of lncRNA *RP11-147L13.8* promotes the invasion ability in NOZ cell lines. Magnification, 200×. Data represent mean ± SEM (three biological replicates). Paired Student's t test. *$p < 0.05$; **$p < 0.001$; ***$p < 0.0001$. (E) The downregulation of lncRNA *RP11-147L13.8* promotes the drug-resistant ability in GBC-SD cell lines. Data represent mean ± SEM (three biological replicates). Paired Student's t test. *$p < 0.05$; **$p < 0.001$; ***$p < 0.0001$. (F) The overexpression of lncRNA *RP11-147L13.8* suppressed the drug-resistant ability in NOZ cell lines. Data represent mean ± SEM (three biological replicates). Paired Student's t test. *$p < 0.05$; **$p < 0.001$; ***$p < 0.0001$.

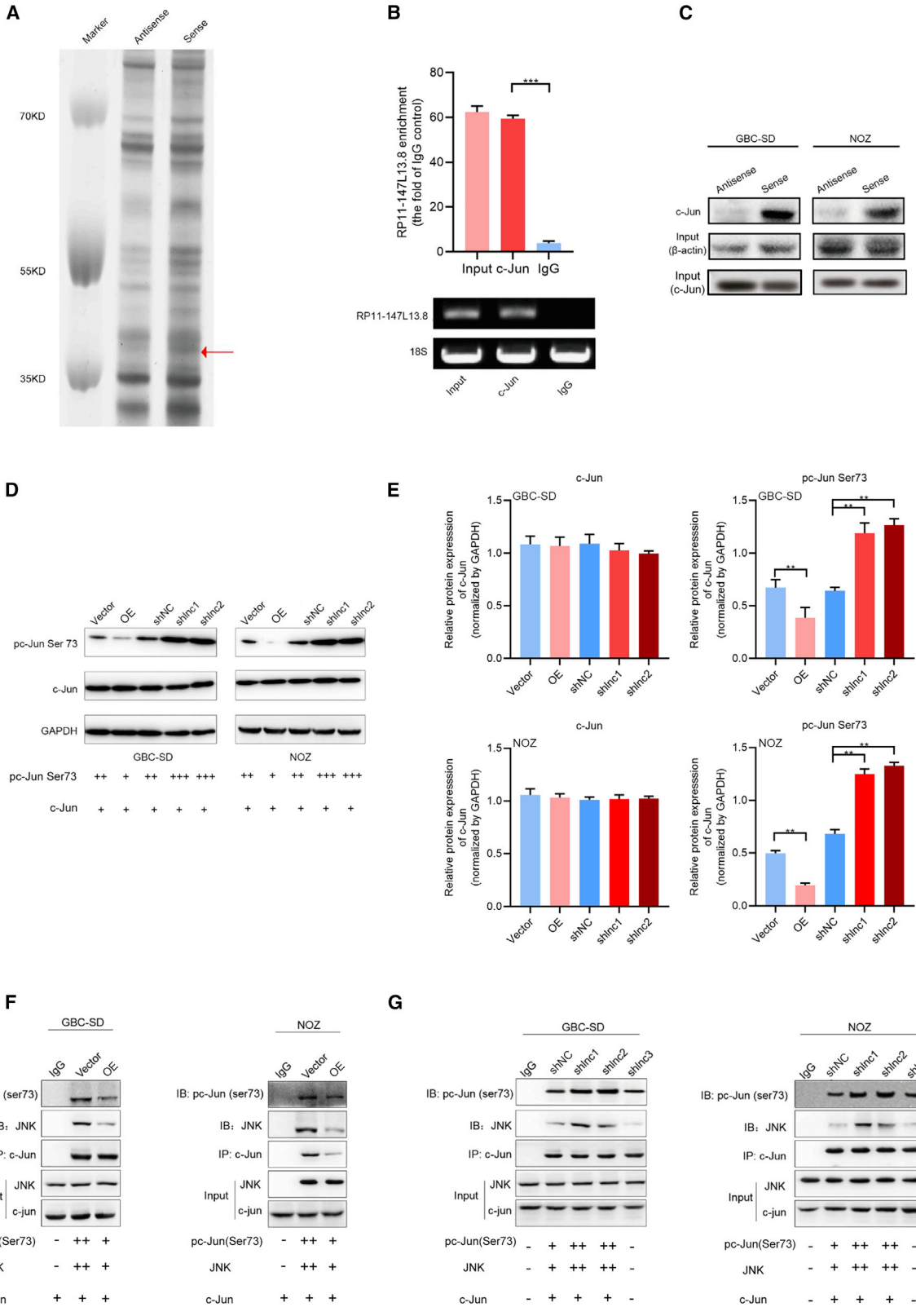

(legend on next page)

node metastasis rate and predicted poorer overall survival rates in patients with GBC. As for the biological role, *RP11-147L13.8* showed strong tumor suppressor activity through suppressing GBC tumor migration and invasion *in vitro*, suggesting that this lncRNA might inhibit the metastasis of GBC. In terms of mechanism, this lncRNA might suppress the c-Jun-ser73 phosphorylation via binding with the delta bZIP domain of c-Jun in GBC to induce its suppressing function.

Currently, numerous studies indicated that lncRNAs could serve as prognostic biomarkers for GBC patients.[25,26] Consistent with previous studies, in our study, we observed that the higher expression level of this lncRNA was positively associated with earlier TNM stage and better overall survival, indicating that this lncRNA might be a potential prognostic biomarker in GBC.

Recently, emerging evidence indicated that lncRNAs play an important role in regulating the progression of GBC. For instance, lncRNA *GBCDRlnc1* might induce chemo-resistance of GBC cells through activating autophagy. Additionally, lncRNA *HGBC* stabilized by Human antigen R (HuR) promotes GBC progression by regulating the miR-502-3p/SET/protein kinase B (AKT) axis.[27] Consistent with these studies, we found that the overexpression of the novel lncRNA *RP11-147L13.8* played an important role in suppressing the tumor invasion, metastasis, and chemo-resistance in GBC. Several sets of evidence supported our conclusion. At first, this lncRNA was significantly downregulated in GBC tissue, GBC patients with venous invasion, and drug-resistant GBC-SD cells, suggesting that RP11-147L13.8 might be involved in the biological process of GBC. Next, the *in vitro* and *in vivo* experiments indicated that the downregulation of *RP11-147L13.8* was significantly promoted, although the overexpression of *RP11-147L13.8* significantly inhibited migration and invasion abilities of GBC cell lines. In terms of the chemo-resistant ability, we found out that patients with a high expression level of this lncRNA were sensitive to chemotherapy. All these results demonstrated that the aberrant expression of this lncRNA could regulate the progression, metastasis, and chemo-resistance of chemotherapy.

The lncRNA could exert its biological function through binding with specific protein or transcription factors. For instance, the interaction of *FAL1* with *BMI1*, an essential subunit of *PRC1*, regulates its protein stability. Another lncRNA, lnc-dendritic cells (lnc-DCs) binds to the transcription factor signal transducer and activator of transcription (STAT3) in the cytoplasm and prevents its dephosphorylation by SH2-containing protein tyrosine phos-phatase-1 (SHP1), thereby activating STAT3 and thus dendritic cell differentiation. In our study, to figure out the underlying mechanism of the biological function of *RP11-147L13.8*, pull-down assay, RIP, and coIP experiments were performed, which indicated that this lncRNA might exert its function via interacting with the bZip domain of the c-Jun protein, which resulted in the suppression of c-Jun-ser73 phosphorylation of c-Jun protein through competitively inhibiting the interaction between the JNK and c-Jun protein. The phosphorylation of c-Jun on Ser73 could also promote tumorigenesis in breast cancer.[28] These results might explain the biological role of this lncRNA. However, further investigation was needed to explain how the c-Jun protein regulates the biological features of GBC.

Among the treatments, gemcitabine is recommended as adjuvant therapy for patients with advanced-stage GBC in clinical practice.[29,30] However, resistance to gemcitabine is often observed and tightly associated with dismal prognosis in GBC.[6] Moreover, lncRNA has been reported in the studies of gemcitabine resistance in GBC.[17,31] In our study, our IC_{50} analysis revealed that *RP11-147L13.8* could enhance the drug sensitivity of gemcitabine in GBC-SD and NOZ cells. Besides, our results indicated that *RP11-147L13.8* exerted its impact on gemcitabine resistance through regulating the phosphorylation of the c-Jun protein. Previously, several studies reported that c-Jun protein played an important role in inducing the drug resistance of gemcitabine resistance, including breast cancer, pancreatic cancer, and bladder cancer.[32–35] All these studies further supported our findings. This suggested that the combinatorial use of gemcitabine and *RP11-147L13.8* transcriptional promoters might produce better therapeutic effects for advanced-stage GBC patients, which shed new insights into the clinical treatment for GBC patients.

In conclusion, our study demonstrated that *RP11-147L13.8* might serve as a tumor-suppressing gene and a prognostic biomarker in GBC, which could inhibit the migration, invasion, and chemo-resistance ability of GBC cells via modulating the phosphorylation of the c-Jun protein, thus providing a potential therapeutic target for GBC treatment.

MATERIALS AND METHODS

Cell lines and human clinical samples

The human GBC cell line GBC-SD was purchased from the Type Culture Collection of the Chinese Academy of Sciences (Shanghai,

Figure 4. *RP11-147L13.8*interacts with c-Jun and suppresses the c-Jun-ser73 phosphorylation via inhibiting the JNK in GBC cells

(A) *RP11-147L13.8* pull-down assay analyzed by SDS-PAGE. (B) The *RP11-147L13.8*-c-Jun interaction was verified by RNA immunoprecipitation (RIP) assays, wherein RP11-147L13.8 was significantly enriched in c-Jun antibody, but not IgG control. (C) The western blot results, which confirmed that c-Jun protein was specifically associated with sense, but not anti-sense, *RP11-147L13.8* in both GBC-SD and NOZ cell lines are shown. (D and E) The overexpression of *RP11-147l13.8* could suppress the ser73 phosphorylation of the c-Jun protein, although the knockdown of *RP11-147l13.8* could promote the ser73 phosphorylation of the c-Jun protein in both GBC-SD and NOZ cell lines. Data represent mean ± SEM (three biological replicates). (F) The co-immunoprecipitation experiment indicated that the overexpression of *RP11-147L13.8* could competitively inhibit the interaction between the JNK and c-Jun protein, which results in the ser73 dephosphorylation of c-Jun protein in both GBC-SD and NOZ cell lines. (G) The co-immunoprecipitation experiment indicated that the knockdown of *RP11-147L13.8* could enhance the interaction between the JNK and c-Jun protein, which results in the ser73 phosphorylation of c-Jun protein in both GBC-SD and NOZ cell lines.

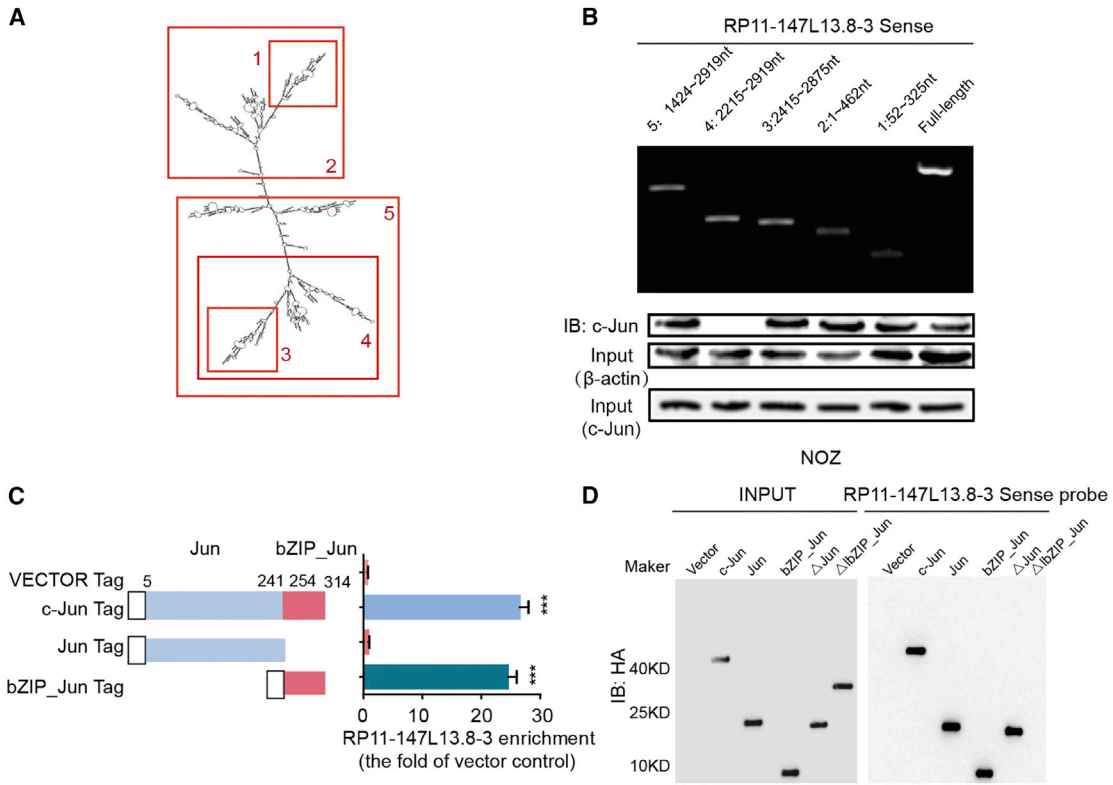

Figure 5. LncRNA RP11-147L13.8 was specifically interacted with the bZIP domain of c-Jun protein

(A) The structure of lncRNA *RP11-147L13.8*. (B) Immunoblotting detection of c-Jun protein in the pull-down samples is shown. The full-length sense biotinylated-RP11-147L13.8 and truncated biotinylated-*RP11-147L13.8* sequence (no. 1 deletes 52–325 bp; no. 2 deletes 1–462 bp; no. 3 deletes 2,415–2,875 bp; no. 4 deletes 2,215–2,919 bp; no. 5 deletes ~1,421–2,919 bp) were analyzed. β-actin and c-Jun serve as input control. (C) The RIP and qPCR results determined the enrichment of *RP11-147L13.8* binding with each c-Jun domain. (D) The pull-down assay and western blot results for different domains of c-Jun protein in NOZ cell lines, which confirmed that lncRNA RP11-147L13.8 specifically interacted with the bZIP domain.

China), although the human GBC cell line NOZ was provided by the Tumor Cytology Research Unit (Medical College, Tongji University, Shanghai, China). Four paired fresh GBC tissues and adjacent non-tumor tissues were collected for the lncRNA microarray analysis, although 96 pairs of fresh GBC tissues and matched adjacent non-tumor tissues from different patients were collected for quantitative reverse-transcriptase PCR (qRT-PCR) analysis. All these patients received surgical resection of their primary tumors in curative intent between 2011 and 2015 at Zhongshan Hospital. All enrolled patients met the following criteria as previously described:[36] (1) they were all pathologically confirmed GBC patients; (2) there was no other anti-cancer treatment history before surgical treatment; (3) there were no concurrence and history of other malignant tumors; (4) all patients had received complete removal of macroscopic tumors and pathological examination had confirmed the negative resection margin; and (5) all patients had complete clinicopathological and follow-up data. The written informed consent was obtained from patients. Ethical approval was obtained from the Zhongshan Hospital Research Ethics Committee and was carried out following the Declaration of Helsinki.

RNA sequencing

The RNA sequencing was performed as previously described.[14] Details were listed in the supplemental information.

Differential expression analysis

The gene read counts of samples in four paired tumor and adjacent normal were used for differential expression analysis. The DESeq2 was implicated to carry out the analysis. In the differential analysis, lncRNA genes with false discovery rate (FDR) $\leq$ 0.05 (Benjamini-Hochberg corrected p value) and $|\log2$ fold-change$| \geq 1$ were determined as significantly differentially expressed genes. The enriched biological themes were identified by using the Database for Annotation, Visualization, and Integrated Discovery (DAVID).[37,38]

Quantitative real-time PCR assay

The TRIzol reagent (Invitrogen, Carlsbad, CA, USA) was used to extract the total RNA of the clinical tissue and cell lines in this study. According to the instructions of the reverse transcriptase kit (Takara Bio, Dalian, China), the total RNA was reverse transcribed into cDNA in the LifePro Thermal Cycler (Hangzhou Bioer Technology,

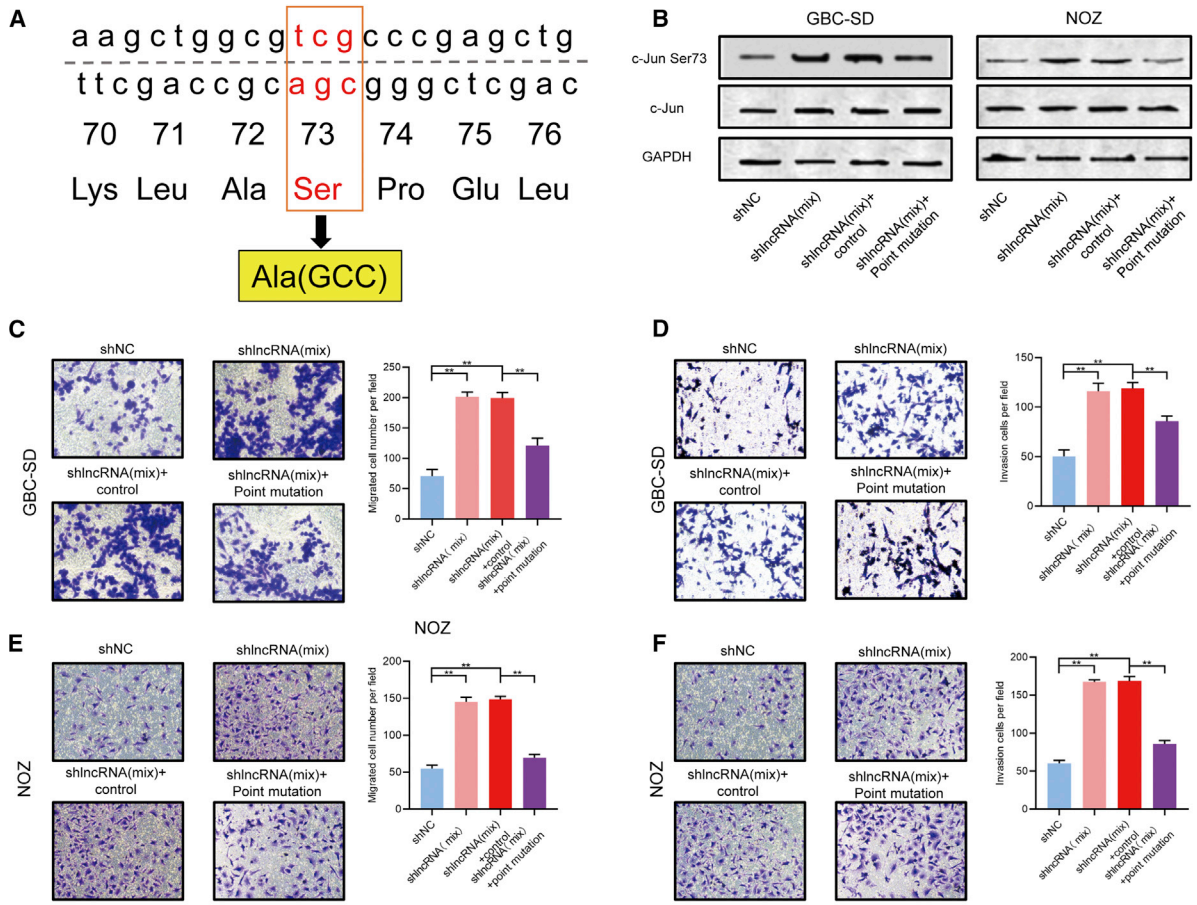

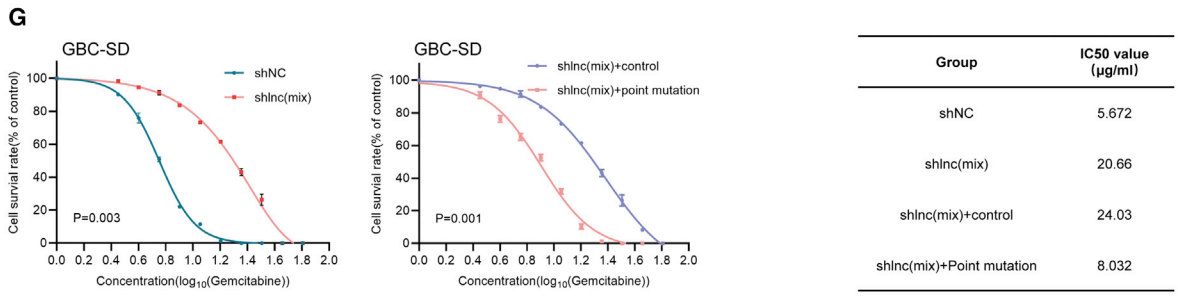

Group	IC50 value (μg/ml)
shNC	5.672
shlnc(mix)	20.66
shlnc(mix)+control	24.03
shlnc(mix)+Point mutation	8.032

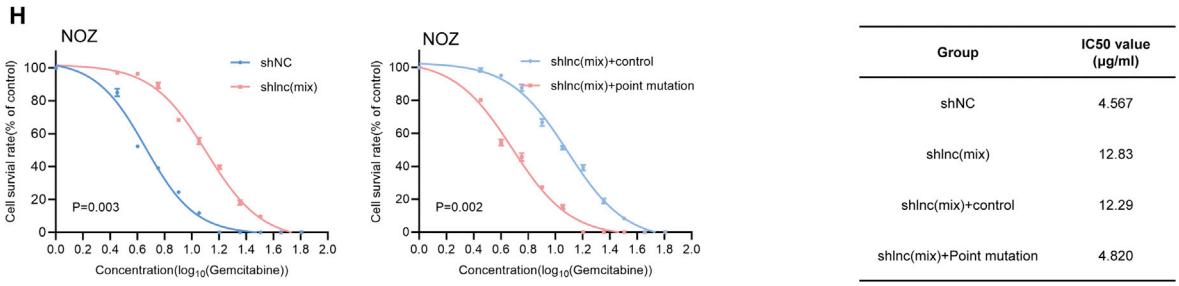

Group	IC50 value (μg/ml)
shNC	4.567
shlnc(mix)	12.83
shlnc(mix)+control	12.29
shlnc(mix)+Point mutation	4.820

(legend on next page)

Hangzhou, China). The qRT-PCR was utilized to determine relative RNA levels, which were measured through a 7900 Real-Time PCR System with the SDS 2.3 software sequence detection system (Applied Biosystem, USE) using the SYBR Green (Takara) method. β-actin was employed as an internal control to normalize the relative RNA levels in each sample and then the relative RNA levels were calculated by utilizing the $2^{-\Delta\Delta Ct}$ relative quantification method.[39] The primer used for this experiment was listed in Table S1.

Northern blot assays and western blot assays

The details of northern blot assays and western blot assays were listed in the supplemental information.

IHC and analysis

The IHC and analysis were carried out as previously described.[40] Quantification criteria of IHC staining were the same as the previous study by two independent pathologists.[41]

RNA interference and lentivirus construction

The details of RNA interference and lentivirus construction were listed in the supplemental information.

In vitro cell migration and invasion assays and *in vivo* metastasis assays

The details of *in vitro* cell migration and invasion assays and *in vivo* metastasis assays were listed in the supplemental information.

In vitro cellular IC_{50} assays

The sh-*RP11-147L13.8* GBC-SD cells, pCDH *RP11-147L13.8* NOZ cells, and corresponding vector cells were seeded in the flat-bottomed plates (96 wells). Ten concentration gradients of gemcitabine were performed to determine the half-maximal inhibitory concentrations that inhibit cell viability (IC_{50} values) in 100 μL suspended cells (5,000 cells) in each plate well. After 48 h culture, the CCK-8 assays (Dojindo, Kyushu, Japan) were employed to evaluate the cell viability.

RNA pull-down assays, mass spectrometry analyses, and RIP assays

To explore the underlying mechanism of *RP11-147L13.8*, RNA pull-down assay, mass spectrometry analyses, and RIP assays were performed. The details of the experiments were presented in the supplemental information.

Immunoblotting analysis and coIP

Immunoprecipitation was carried out as described previously.[42] Details of the immunoblotting analysis and coIP were listed in the supplemental information.

Survival analysis

Survival analysis was performed as described in a previous study.[43]

Statistical analysis

Data were displayed in the mean ± SEM (standard error of the mean) or median with interquartile range form. The Student's t test or Wilcoxon signed-rank test was used to evaluate the differences between the two groups. The correlation between *RP11-147L13.8* RNA levels and overall survival of GBC patients was estimated via the log rank test. Besides, the chi-square test was carried out to assess the functional impact of *RP11-147L13.8* on GBC cell lines metastasis *in vivo*. All statistical calculations in this study were performed in the R environment. Unless specially stated, a two-tailed $p < 0.05$ is considered statistically significant.

SUPPLEMENTAL INFORMATION

Supplemental information can be found online at https://doi.org/10.1016/j.omto.2021.08.016.

ACKNOWLEDGMENTS

This study was supported by grants from the National Natural Science Foundation of China (81872352 and82072682), Shanghai Top Priority Clinical Medical Center and Key Discipline Construction Plan (2017ZZ02007), Natural Science Foundation of Shanghai (21ZR1459100), and Science and Technology Commission of

Figure 6. The rescue assay confirmed that lncRNA RP11-147L13.8 performs its biological function through suppressing the c-Jun-ser73 phosphorylation in GBC cell lines

(A) The strategy of the point mutation. The Ser at 73 sites of JUN was changed into Ala. (B) After transfection, the phosphorylation of c-Jun has been suppressed in both GBC-SD and NOZ cell lines (three biological replicates). (C) After the knockdown of lncRNA, the migration ability of GBC-SD has been promoted, although after the point mutation, the migration ability of the knockdown GBC-SD has been suppressed. Magnification, 200×. Data represent mean ± SEM (three biological replicates). *$p < 0.05$; **$p < 0.001$; ***$p < 0.0001$. (D) After the knockdown of lncRNA, the invasion ability of GBC-SD has been promoted, although after the point mutation, the invasion ability of the knockdown GBC-SD has been suppressed. Magnification, 200×. Data represent mean ± SEM (three biological replicates). *$p < 0.05$; **$p < 0.001$; ***$p < 0.0001$. (E) After the knockdown of lncRNA, the migration ability of NOZ has been promoted, although after the point mutation, the migration ability of the knockdown GBC-SD has been suppressed. Magnification, 200×. Data represent mean ± SEM (three biological replicates). *$p < 0.05$; **$p < 0.001$; ***$p < 0.0001$. (F) After the knockdown of lncRNA, the invasion ability of NOZ has been promoted, although after the point mutation, the invasion ability of the knockdown GBC-SD has been suppressed. Magnification, 200×. Data represent mean ± SEM (three biological replicates). *$p < 0.05$; **$p < 0.001$; ***$p < 0.0001$. (G) After the knockdown of lncRNA, the IC_{50} value of GBC-SD for gemcitabine was significantly upregulated (shNC versus shlnc(mix): 5.672 μg/mL versus 20.66 μg/mL). After the point mutation, the IC_{50} value of GBC-SD for gemcitabine was significantly decreased (shlnc(mix)+control versus shlnc(mix)+point mutation: 24.03 μg/mL versus 8.032 μg/mL). Data represent mean ± SEM (three biological replicates). Student's t test. (H) After the knockdown of lncRNA, the IC_{50} value of NOZ for gemcitabine was significantly upregulated (shNC versus shlnc(mix): 4.567 μg/mL versus 12.830 μg/mL). After the point mutation, the IC_{50} value of GBC-SD for gemcitabine was significantly decreased (shlnc(mix)+control versus shlnc(mix)+point mutation: 12.29 versus 4.820 μg/mL). Data represent mean ± SEM (three biological replicates). Student's t test.

Shanghai Municipality (20DZ2254500). We thank Prof. Jiwei Zhang for his assistance in this manuscript.

AUTHOR CONTRIBUTIONS

Houbao Liu, Han Liu, and S.S. designed and supervised the study. B.Z., J.W., W.S., K.F., and W.W. performed data analysis and functional experiments. Xiaojian Ni, Z.G., D.Z., Xiaoling Ni, and T.S. collected and managed patient samples. S.S., Houbao Liu, Han Liu, and B.Z. wrote and reviewed the manuscript. All authors read and approved the final manuscript.

DECLARATION OF INTERESTS

The authors declare no competing interests.

REFERENCES

1. Henley, S.J., Weir, H.K., Jim, M.A., Watson, M., and Richardson, L.C. (2015). Gallbladder cancer incidence and mortality, United States 1999-2011. Cancer Epidemiol. Biomarkers Prev. *24*, 1319–1326.
2. Siegel, R.L., Miller, K.D., and Jemal, A. (2020). Cancer statistics, 2020. CA Cancer J. Clin. *70*, 7–30.
3. Misra, S.P., and Dwivedi, M. (1990). Pancreaticobiliary ductal union. Gut *31*, 1144–1149.
4. Shindoh, J., de Aretxabala, X., Aloia, T.A., Roa, J.C., Roa, I., Zimmitti, G., Javle, M., Conrad, C., Maru, D.M., Aoki, T., et al. (2015). Tumor location is a strong predictor of tumor progression and survival in T2 gallbladder cancer: an international multicenter study. Ann. Surg. *261*, 733–739.
5. Horgan, A.M., Amir, E., Walter, T., and Knox, J.J. (2012). Adjuvant therapy in the treatment of biliary tract cancer: a systematic review and meta-analysis. J. Clin. Oncol. *30*, 1934–1940.
6. Goetze, T.O. (2015). Gallbladder carcinoma: prognostic factors and therapeutic options. World J. Gastroenterol. *21*, 12211–12217.
7. Gutschner, T., and Diederichs, S. (2012). The hallmarks of cancer: a long non-coding RNA point of view. RNA Biol. *9*, 703–719.
8. Gibb, E.A., Brown, C.J., and Lam, W.L. (2011). The functional role of long non-coding RNA in human carcinomas. Mol. Cancer *10*, 38.
9. Gupta, R.A., Shah, N., Wang, K.C., Kim, J., Horlings, H.M., Wong, D.J., Tsai, M.C., Hung, T., Argani, P., Rinn, J.L., et al. (2010). Long non-coding RNA HOTAIR reprograms chromatin state to promote cancer metastasis. Nature *464*, 1071–1076.
10. Tsai, M.C., Manor, O., Wan, Y., Mosammaparast, N., Wang, J.K., Lan, F., Shi, Y., Segal, E., and Chang, H.Y. (2010). Long noncoding RNA as modular scaffold of histone modification complexes. Science *329*, 689–693.
11. Wang, L., Bu, P., Ai, Y., Srinivasan, T., Chen, H.J., Xiang, K., Lipkin, S.M., and Shen, X. (2016). A long non-coding RNA targets microRNA miR-34a to regulate colon cancer stem cell asymmetric division. eLife *5*, e14620.
12. Ni, W., Yao, S., Zhou, Y., Liu, Y., Huang, P., Zhou, A., Liu, J., Che, L., and Li, J. (2019). Long noncoding RNA GAS5 inhibits progression of colorectal cancer by interacting with and triggering YAP phosphorylation and degradation and is negatively regulated by the m^6A reader YTHDF3. Mol. Cancer *18*, 143.
13. Qin, G., Tu, X., Li, H., Cao, P., Chen, X., Song, J., Han, H., Li, Y., Guo, B., Yang, L., et al. (2020). Long noncoding RNA p53-stabilizing and activating RNA promotes p53 signaling by inhibiting heterogeneous nuclear ribonucleoprotein K deSUMOylation and suppresses hepatocellular carcinoma. Hepatology *71*, 112–129.
14. Shen, S., Wang, J., Zheng, B., Tao, Y., Li, M., Wang, Y., Ni, X., Suo, T., Liu, H., Liu, H., and Zhang, J. (2020). LINC01714 enhances gemcitabine sensitivity by modulating FOXO3 phosphorylation in cholangiocarcinoma. Mol. Ther. Nucleic Acids *19*, 446–457.
15. Chen, J., Yu, Y., Li, H., Hu, Q., Chen, X., He, Y., Xue, C., Ren, F., Ren, Z., Li, J., et al. (2019). Long non-coding RNA PVT1 promotes tumor progression by regulating the miR-143/HK2 axis in gallbladder cancer. Mol. Cancer *18*, 33.
16. Wang, S.H., Ma, F., Tang, Z.H., Wu, X.C., Cai, Q., Zhang, M.D., Weng, M.Z., Zhou, D., Wang, J.D., and Quan, Z.W. (2016). Long non-coding RNA H19 regulates FOXM1 expression by competitively binding endogenous miR-342-3p in gallbladder cancer. J. Exp. Clin. Cancer Res. *35*, 160.
17. Cai, Q., Wang, S., Jin, L., Weng, M., Zhou, D., Wang, J., Tang, Z., and Quan, Z. (2019). Long non-coding RNA GBCDRlnc1 induces chemoresistance of gallbladder cancer cells by activating autophagy. Mol. Cancer *18*, 82.
18. Vogt, P.K. (2002). Fortuitous convergences: the beginnings of JUN. Nat. Rev. Cancer *2*, 465–469.
19. Hoeffler, W.K., Levinson, A.D., and Bauer, E.A. (1994). Activation of c-Jun transcription factor by substitution of a charged residue in its N-terminal domain. Nucleic Acids Res. *22*, 1305–1312.
20. Mishra, R.K., Potteti, H.R., Tamatam, C.R., Elangovan, I., and Reddy, S.P. (2016). c-Jun is required for nuclear factor-κB-dependent, LPS-stimulated Fos-related antigen-1 transcription in alveolar macrophages. Am. J. Respir. Cell Mol. Biol. *55*, 667–674.
21. Yang, L., Liu, C.C., Zheng, H., Kanekiyo, T., Atagi, Y., Jia, L., Wang, D., N'songo, A., Can, D., Xu, H., et al. (2016). LRP1 modulates the microglial immune response via regulation of JNK and NF-κB signaling pathways. J. Neuroinflammation *13*, 304.
22. Roszak, J., Smok-Pieniążek, A., and Stępnik, M. (2017). Transcriptomic analysis of the PI3K/Akt signaling pathway reveals the dual role of the c-Jun oncogene in cytotoxicity and the development of resistance in HL-60 leukemia cells in response to arsenic trioxide. Adv. Clin. Exp. Med. *26*, 1335–1342.
23. Volders, P.J., Helsens, K., Wang, X., Menten, B., Martens, L., Gevaert, K., Vandesompele, J., and Mestdagh, P. (2013). LNCipedia: a database for annotated human lncRNA transcript sequences and structures. Nucleic Acids Res. *41*, D246–D251.
24. Wang, L., Park, H.J., Dasari, S., Wang, S., Kocher, J.P., and Li, W. (2013). CPAT: Coding-Potential Assessment Tool using an alignment-free logistic regression model. Nucleic Acids Res. *41*, e74.
25. Wang, S.H., Wu, X.C., Zhang, M.D., Weng, M.Z., Zhou, D., and Quan, Z.W. (2015). Upregulation of H19 indicates a poor prognosis in gallbladder carcinoma and promotes epithelial-mesenchymal transition. Am. J. Cancer Res. *6*, 15–26.
26. Wu, X.S., Wang, X.A., Wu, W.G., Hu, Y.P., Li, M.L., Ding, Q., Weng, H., Shu, Y.J., Liu, T.Y., Jiang, L., et al. (2014). MALAT1 promotes the proliferation and metastasis of gallbladder cancer cells by activating the ERK/MAPK pathway. Cancer Biol. Ther. *15*, 806–814.
27. Hu, Y.P., Jin, Y.P., Wu, X.S., Yang, Y., Li, Y.S., Li, H.F., Xiang, S.S., Song, X.L., Jiang, L., Zhang, Y.J., et al. (2019). LncRNA-HGBC stabilized by HuR promotes gallbladder cancer progression by regulating miR-502-3p/SET/AKT axis. Mol. Cancer *18*, 167.
28. Zhang, Y., Baysac, K.C., Yee, L.F., Saporita, A.J., and Weber, J.D. (2014). Elevated DDX21 regulates c-Jun activity and rRNA processing in human breast cancers. Breast Cancer Res. *16*, 449.
29. Lee, D.G., Lee, S.H., Kim, J.S., Park, J., Cho, Y.L., Kim, K.S., Jo, D.Y., Song, I.C., Kim, N., Yun, H.J., et al. (2015). Loss of NDRG2 promotes epithelial-mesenchymal transition of gallbladder carcinoma cells through MMP-19-mediated Slug expression. J. Hepatol. *63*, 1429–1439.
30. Xu, S., Zhan, M., Jiang, C., He, M., Yang, L., Shen, H., Huang, S., Huang, X., Lin, R., Shi, Y., et al. (2019). Genome-wide CRISPR screen identifies ELP5 as a determinant of gemcitabine sensitivity in gallbladder cancer. Nat. Commun. *10*, 5492.
31. Xue, Z., Yang, B., Xu, Q., Zhu, X., and Qin, G. (2020). Long non-coding RNA SSTR5-AS1 facilitates gemcitabine resistance via stabilizing NONO in gallbladder carcinoma. Biochem. Biophys. Res. Commun. *522*, 952–959.
32. Huang, X.L., Zhang, H., Yang, X.Y., Dong, X.Y., Xie, X.Y., Yin, H.B., Gou, X., Lin, Y., and He, W.Y. (2017). Activation of a c-Jun N-terminal kinase-mediated autophagy pathway attenuates the anticancer activity of gemcitabine in human bladder cancer cells. Anticancer Drugs *28*, 596–602.
33. Ren, X., Zhao, W., Du, Y., Zhang, T., You, L., and Zhao, Y. (2016). Activator protein 1 promotes gemcitabine-induced apoptosis in pancreatic cancer by upregulating its downstream target Bim. Oncol. Lett. *12*, 4732–4738.

34. Tu, M., Li, H., Lv, N., Xi, C., Lu, Z., Wei, J., Chen, J., Guo, F., Jiang, K., Song, G., et al. (2017). Vasohibin 2 reduces chemosensitivity to gemcitabine in pancreatic cancer cells via Jun proto-oncogene dependent transactivation of ribonucleotide reductase regulatory subunit M2. Mol. Cancer *16*, 66.

35. Wu, Z.H., Lin, C., Liu, M.M., Zhang, J., Tao, Z.H., and Hu, X.C. (2016). Src inhibition can synergize with gemcitabine and reverse resistance in triple negative breast cancer cells via the AKT/c-Jun pathway. PLoS ONE *11*, e0169230.

36. Shen, S., Wang, J.W., Zheng, B.H., Ni, X.J., Gao, Z.H., Zhang, D.X., Lu, P.X., Ni, X.L., Suo, T., Liu, H.B., and Liu, H. (2020). The lnc-CITED2-2:1 inhibits metastasis via inhibiting CITED2 and epithelial-mesenchymal transition in gallbladder cancer. Clin. Transl. Med. *10*, e116.

37. Huang, W., Sherman, B.T., and Lempicki, R.A. (2009). Systematic and integrative analysis of large gene lists using DAVID bioinformatics resources. Nat. Protoc. *4*, 44–57.

38. Huang, W., Sherman, B.T., and Lempicki, R.A. (2009). Bioinformatics enrichment tools: paths toward the comprehensive functional analysis of large gene lists. Nucleic Acids Res. *37*, 1–13.

39. Li, Z., Zhang, J., Liu, X., Li, S., Wang, Q., Di Chen, Hu, Z., Yu, T., Ding, J., Li, J., et al. (2018). The LINC01138 drives malignancies via activating arginine methyltransferase 5 in hepatocellular carcinoma. Nat. Commun. *9*, 1572.

40. Liu, L.Z., Zhang, Z., Zheng, B.H., Shi, Y., Duan, M., Ma, L.J., Wang, Z.C., Dong, L.Q., Dong, P.P., Shi, J.Y., et al. (2019). CCL15 recruits suppressive monocytes to facilitate immune escape and disease progression in hepatocellular carcinoma. Hepatology *69*, 143–159.

41. Duan, F., Wu, H., Jia, D., Wu, W., Ren, S., Wang, L., Song, S., Guo, X., Liu, F., Ruan, Y., and Gu, J. (2018). O-GlcNAcylation of RACK1 promotes hepatocellular carcinogenesis. J. Hepatol. *68*, 1191–1202.

42. Fan, K., Zhang, D., Li, M., Shen, S., Wang, J., Ni, X., Gong, Z., Zheng, B., Gao, Z., Ni, X., et al. (2020). Carboxyl-terminal polypeptide fragment of MUC16 combing stathmin1 promotes gallbladder cancer cell migration and invasion. Med. Oncol. *37*, 114.

43. Zheng, B.H., Ma, J.Q., Tian, L.Y., Dong, L.Q., Song, G.H., Pan, J.M., Liu, Y.M., Yang, S.X., Wang, X.Y., Zhang, X.M., et al. (2020). The distribution of immune cells within combined hepatocellular carcinoma and cholangiocarcinoma predicts clinical outcome. Clin. Transl. Med. *10*, 45–56.

OMTO, Volume *23*

Supplemental information

lncRNA *RP11-147L13.8* suppresses metastasis and chemo-resistance by modulating the phosphorylation of c-Jun protein in GBC

Bohao Zheng, Jiwen Wang, Kun Fan, Wentao Sun, Wenze Wan, Zhihui Gao, Xiaojian Ni, Dexiang Zhang, Xiaoling Ni, Tao Suo, Han Liu, Houbao Liu, and Sheng Shen

Supplementary Figures

Figure S1 The validation of top ten down-regulated long non-coding RNA.
A: The volcano map presented the top ten upregulation (red spot) and downregulation (blue spot) long non-coding RNA in gallbladder cancer. Data represent mean ± s.e.m. (Three biological replicates).
B: The list of the top ten upregulation and downregulation long non-coding RNA in gallbladder cancer.
C: The qPCR results validated that RP-11147L13.8 was significantly downregulated in the 24 pairs of GBC tissues.

Figure S2 LNCipedia and CPAT databases indicate that there is no protein-coding ability for RP11-147L13.8.

Figure S3 The basic information of RP11-147L13.8 and the establishment of the stable knockdown and overexpression GBC cells.
A: The expression level of *RP11-147L13.8* among different kinds of tumors and human tissues.
B: The identification of full-length *RP11-147L13.8* in GBC-SD cells. Representative images and the boundary of the PCR products from 5' RACE and 3' RACE were shown.
C: The expression levels of *RP11-147L13.8* in different GBC cell lines, including GBC-SD, SGC-996, G-415, TGBC2TKB, TGBC24TKB, and NOZ cell lines.
D: The distribution of *RP11-147L13.8* in cyto-plasma (35%) and nucleus (65%) of GBC-SD cell lines. β-actin serves as a cytoplasmic marker, while U6 serves as a nuclear marker. Values are shown as mean ± S.E.M.
E: qPCR results indicated the altered expression level of RP11-147L13.8 in different groups of cell lines (Vector, OE, shNC, shlnc1, shlnc2, shlnc3).

Figure S4 *RP11-147L13.8* could significantly suppress the metastasis of GBC in vivo.
A: The tumor formation was observed 7 days after the injection of the cell lines. No significant differences were observed in the tumor volume. Data represent mean ± s.e.m. Student's t-test. *P<0.05; **P<0.001; ***P<0.0001.
B: No significant differences were observed in the tumor weight. Data represent mean ± s.e.m. Student's t-test. *P<0.05; **P<0.001; ***P<0.0001.
C: Representative images of H&E staining in the metastatic liver loci and statistical data comparing the knockdown group with the control group. (n=6)
D: Representative images of H&E staining in the metastatic lung loci and statistical data comparing the knockdown group with the control group. (n=6)

Figure S5 The correlation between the RP11-147l13.8 and the expression level of c-Jun-ser73 protein and the prognostic significance of c-Jun protein.

A: The typical immunohistochemistry image of the low and high expression of c-Jun-ser73 in gallbladder cancer tissue. (magnification:×200)

B: Patients with high expression levels of c-Jun-ser73 (red line) were associated with poorer overall survival. (Log-rank test, P=0.03).

C: The expression level of RP11-147L13.8 was negatively correlated with the expression level of c-Jun-ser73(R=; P=0.002). Spearman correlation analysis.

Figure S6 A mechanistic model for the function of RP11-147L13.8 in gallbladder cancer.

Figure S1

A

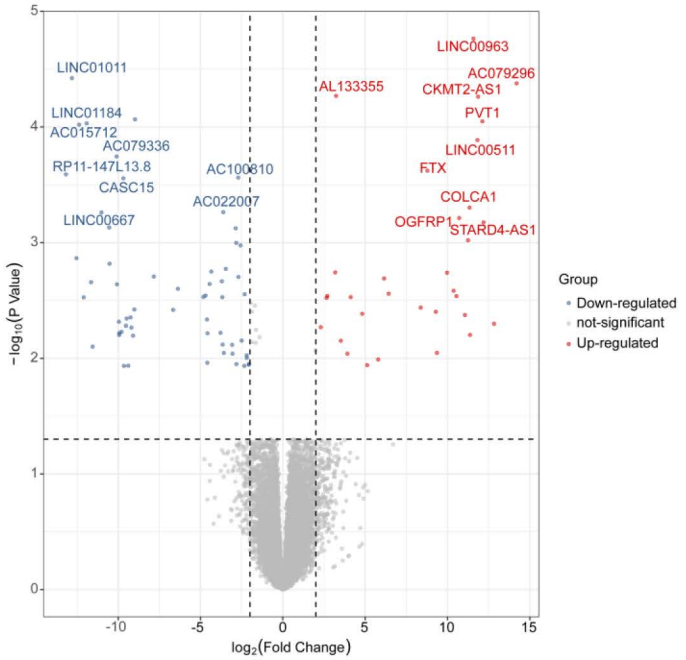

B

Top ten up-regulation and down-regulation long non coding RNA in gallbladder cancer

Seq Name	Gene name	Log_2(Fc)	P value	Regulation	Significant
ENST00000419300	LINC00963	11.58	0.00	up	yes
ENST00000670061	AC079296	14.19	0.00	up	yes
ENST00000670957	CKMT2-AS1	11.86	0.00	up	yes
ENST00000661988	PVT1	12.12	0.00	up	yes
ENST00000650423	LINC00511	11.82	0.00	up	yes
ENST00000669257	COLCA1	11.34	0.00	up	yes
ENST00000654777	STARD4-AS1	12.19	0.00	up	yes
ENST00000504145	AF117829	11.25	0.00	up	yes
ENST00000609067	AC084018	12.83	0.01	up	yes
ENST00000651019	AC068282	11.37	0.01	up	yes
ENSG00000267731	**RP11-147L13.8**	**-12.82**	**0.00**	**down**	**yes**
ENST00000663841	LINC01184	-11.92	0.00	down	yes
ENST00000560068	AC015712	-12.38	0.00	down	yes
ENST00000655321	AC009242	-13.18	0.00	down	yes
ENST00000654021	LINC00667	-11.02	0.00	down	yes
ENST00000474768	ADAMTS9-AS2	-10.55	0.00	down	yes
ENST00000453136	AC234582	-12.54	0.00	down	yes
ENST00000412639	LNCTAM34A	-11.65	0.00	down	yes
ENST00000403969	RNF216P1	-12.10	0.00	down	yes
ENST00000366437	MIR205HG	-11.56	0.01	down	yes

C

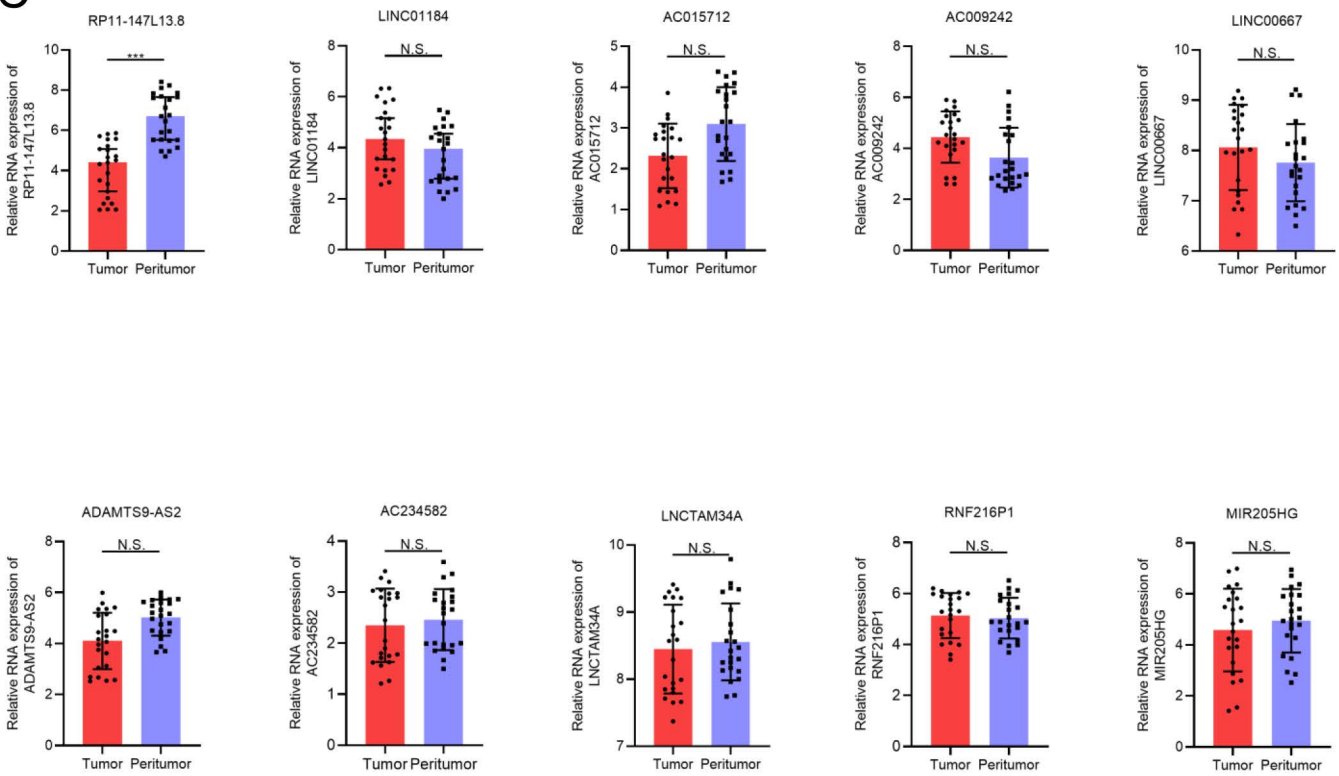

Figure S2

CPAT analysis of RP11-147L13.8

Calculator User Guide Feedback Source Code

Result for species name : hg19 with job ID :1626712581

Data ID	Sequence Name	RNA Size	ORF Size	Ficket Score	Hexamer Score	Coding Probability	Coding Label
0	RP11-147L13.8	2919	336	0.757	-0.150597546964	0.037066854677152	no

This job has been stored with the job ID
Download Table in tab delimetered file (.txt)

For suggestions, comments or queries about this website, please leave your feedback through Feedback.

BCM Baylor College of Medicine MAYO CLINIC

RNA sequence data of RP11-147L13.8

AGGACTTTGAAGACCCAAGCAGCCAAAAAATAGCTAATTCCTCCTTATTTCAGTTGGTATGAAGAGAAGGTTACTAATAATGCTGCTCTTCCAGC
ACAAGTCTTCTGGGCTGTCAGTGAGCTTGGTCAGTGGGAACCACAGGAAATTATGAGTTATGTTTGTTATATATGAGAGGAAAATTGAGGCTACC
AGTCTTGTCACAGGGTTTATAGATAATTGCCTTGTGTGCCACCATGCCTGGATAATTTTTGTATTTTTAGTAGACAGGGGATTTCACCATGTTGGC
CAGGCTGGTCTCAAGCTCCTGACCTCAGGTGATCTGCCTGCCTTGGCCTCCCAAAGTGCTGGGATTACAGGCGTGAGCCACCGCGCCCAGCA
CCCCATTAAATCTTATCACAAAGCCTCTTCAAACTTGGCTCCAATGGAGGGAATTGATACTTCAGCAATATTCTGTCTTCTACTCCATGAGCATAA
ACTGATGCTATCCTGAGCAAACTAGAATGATTACCCTATGAAGGTTCAGTAACTATAATAGGGGTATTTTTGGCATTAGTTTGAGACCTACAGCCT
GTGCCAAAAGTGAACAGGAAGCATCACATTTAAAAGATGTATAAAATATGTCTATATCTATCCATTTGATATGGCTTGACTGTGTCACCACCCAAA
TCTTATTTGGAATTCCCACATGTTGTAGGAGGGAACCGGTAGGAGGTAATTGAATCATGGGGGCAAGTCTCCCGTGCTATTTTCATGATAGTGAA
TAAGTCTCACGATATCTGATGGTTTTAAAAAAAGGAGTTCCCCTGCACAAGCTCTCTGTGTTTGCCTACTGCCATCCATGTAAGACGTGACTTGC
TCCTCCTTGCCTTCTAATACATCATCTATCTGGTTATTTCATACATATTTTCTAGCATTTTATTATTGGTTTCTTCAAAACTCTTCAGAAACTAATATA
TGTATATTTTCCACCATGATCAACTGTGCATATTAATATATATTATTTGGTATATGAATGTGGATTCATAATTGAGATTATGTTCCAATGAGTCATAG
TAAAAGTACAGAAAATTAATATTTCTAATGCCTTATCAACCGATGATTATTATAAAATTAGCCTTTATGTCAAGTTCTCATTGCTCTTGAATTTCATT
CCAAACAGAATTTTGGAATTCATATTATTTGGAATAGTATAGCTGTCATACCTAAATTAGTTTAATAACCCACATCTAATGCAAATTTACATTAAGAT
TTTACATAAATAATTATGGTGTAGAGTATGACAATCCTATTTCAAAACCACAGAGCCCTTAGAAAAACAAATTCTTGATTTTTCAGATATCTCAAAT
ACTGTAAAATACAGTATAACTAAGAATAATTAGCCATGAGGTCAAACTTCAATTTCAAACATTATAAAAGTAAAATTAAGAGTTAAAATCTAAAACC
ACATGAAAATTTATTCTTCATTATAATCTCAAATTTGAAAACGTTATATAAGATTTATGCATTCATTAGAAAGTGATTTATTGTAATTTTATAAGATTT
GCCAATTTTTAAAGGTGTATTTTTGATCAATGCAATTAAATGTTAAAATTATTATGCTATACATTATTAGTTCATGACACATTTTCAAATATGAATGT
GATGTAGAAACAGGTGATTATCAGAAAATAAACTCTGTTTTTAGTTTAAGACTAAATTAAAGCTACCAAAAAGAAATTTAGTTTCAAGATAGGAAA
GTTTATTTGTAAGGATGCTGGGATGTTTGAACCCAAGATGAGTGATGTTTAAAAGGTTTTGCAATGGCATTCAATGAATAAAAAATGTTTAGAGTT
CAGTAACTTCAGTTACCATTTTGGACAGATAACAAGAGATCCAATCTGACTAGCAGAGAATAGTGTAAGACATTTAGAATAGTTAGCAGTTTAAAT
CAGAGGGTAGACAGATTATTTTCCAATGTAGAGTACATATTTCTCCATTTGCATAATCCTCACCAGTGGGTAGAATTTATGAAGAATAGAATTTGG
TTCATGGAAAGAAAAGCAGGCAGGAACTAAATCAGATATAACTTTCTTCATATTTAATAACTGAAGTTTACTCCTATTTTGAGACTCAATTCTGATA
GAAGTTGGAAAATTAATCTGTCAGTTTAACCCTATCTCTAACCCCCTGCCATGTAGAGAATTGAACTAGCCTTCGCTCTCATAAGTGGAATTTTAA
AAAATAATGAGTTACATGAGCTGATAAGCACACATGCATAGTCAATGTTAAGGCTTAGCATTTATAAAATTTGGGATGATAATTTATGGCAAATGT
TTAACACATTTAATAAGATAAATAGTTTTTAAGGCATTGAATAGGTAGGAGTTCATATGAGTTTACTCTGGGTTGCTATTACTTTTACATAGTCAAA
CTTTATTTTGTAGTATTTTTCTTCTTGATTCTCTAGTCACTATGATAATTATTAGTATGGATGGTGACTTTTATTTCCAAGCACAGCATAATCCACAA
TAACATAACATTTAAAAGCAAAGGCTCTGTATCGATTATTAACATGAACAATTTCCTTTGCTACCATACTCCATCCAGATAAAGAACTGAATGTTCC
TCTGAACCTTCCAATTAATTTCCTCCATTGTGATGAATCCTCCATAGATTTATTGGCAAAACATTATTTCTAAGTGTTCTCCACCCTACTATAAATT
GTCTCAAAATAGTTTGTGTCTACCAACAAGGTAGTATAGACTATAAACTTAATAAATAGTAATTATTGATAATTATGAGATACCAGGATGCTAATGA
AACTTTATTGCTTGTATTGAGAAATGAGAGTATAAATTGAGTATAAAATGAAAAGACTTGAATGCTTAGTAAAGCATATAATGTAGCTAAAGTTATT
AAACAGATATATGTATATGCCAA

Lncipedia data of RP11-147L13.8

Protein coding potential

Metric	Raw result	Interpretation
PRIDE reprocessing 2.0	0	non-coding
Lee translation initiation sites	0	non-coding
PhyloCSF score	9.343	non-coding
CPAT coding probability	7.35%	non-coding
Bazzini small ORFs	0	non-coding

In stringent set: **yes**

Figure S3

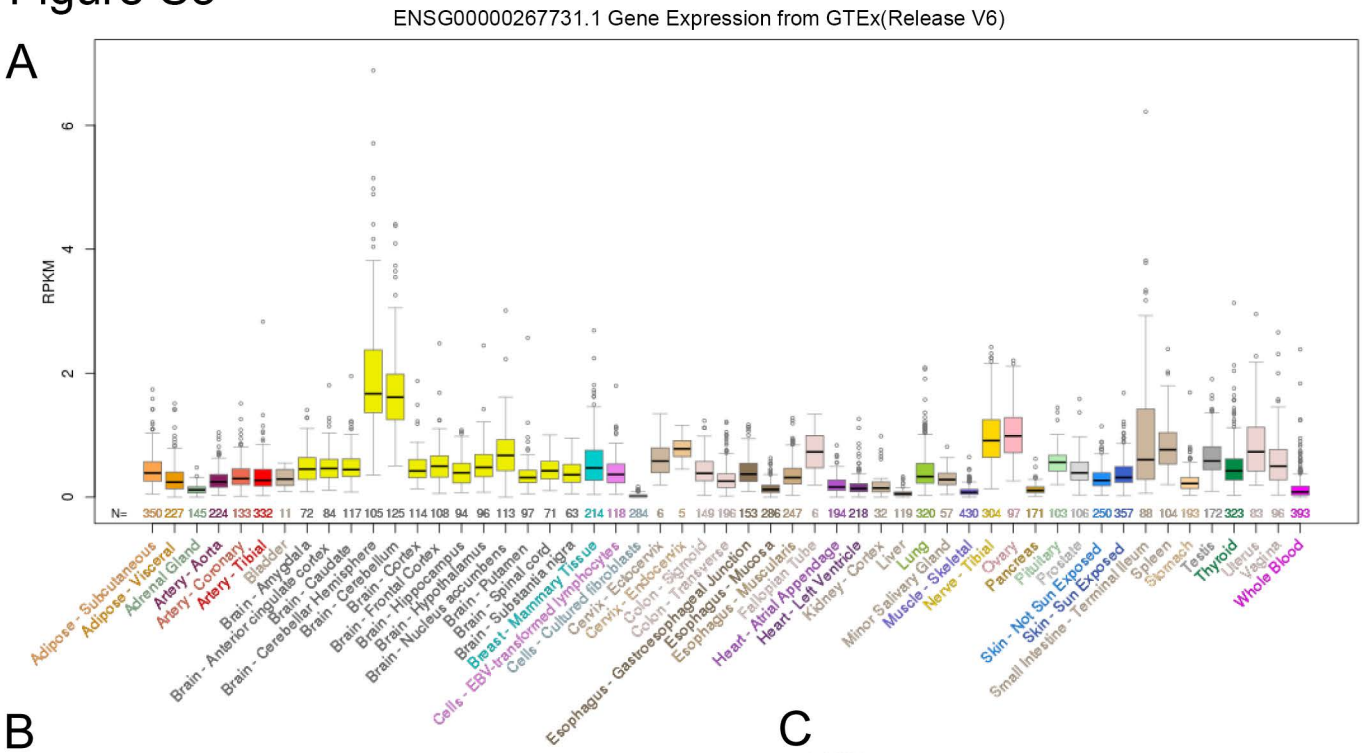
ENSG00000267731.1 Gene Expression from GTEx(Release V6)
A
RPKM
N=
Adipose - Subcutaneous
Adipose - Visceral
Adrenal Gland
Artery - Aorta
Artery - Coronary
Artery - Tibial
Bladder
Brain - Amygdala
Brain - Anterior cingulate cortex
Brain - Caudate
Brain - Cerebellar Hemisphere
Brain - Cerebellum
Brain - Cortex
Brain - Frontal Cortex
Brain - Hippocampus
Brain - Hypothalamus
Brain - Nucleus accumbens
Brain - Putamen
Brain - Spinal cord
Brain - Substantia nigra
Breast - Mammary Tissue
Cells - EBV-transformed lymphocytes
Cells - Cultured fibroblasts
Cervix - Ectocervix
Cervix - Endocervix
Colon - Sigmoid
Colon - Transverse
Esophagus - Gastroesophageal Junction
Esophagus - Mucosa
Esophagus - Muscularis
Fallopian Tube
Heart - Atrial Appendage
Heart - Left Ventricle
Kidney - Cortex
Liver
Lung
Minor Salivary Gland
Muscle - Skeletal
Nerve - Tibial
Ovary
Pancreas
Pituitary
Prostate
Skin - Not Sun Exposed
Skin - Sun Exposed
Small Intestine - Terminal Ileum
Spleen
Stomach
Testis
Thyroid
Uterus
Vagina
Whole Blood

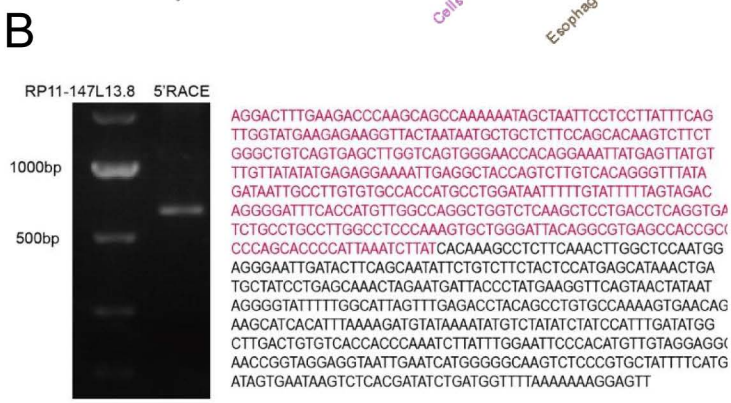
B
RP11-147L13.8 5'RACE
1000bp
500bp
AGGACTTTGAAGACCCAAGCAGCCAAAAAATAGCTAATTCCTCCTTATTTCAG
TTGGTATGAAGAGAAGGTTACTAATAATGCTGCTCTTCCAGCACAAGTCTTCT
GGGCTGTCAGTGAGCTTGGTCAGTGGGAACCACAGGAAATTATGAGTTATGT
TTGTTATATATGAGAGGAAAATTGAGGCTACCAGTCTTGTCACAGGGTTTATA
GATAATTGCCTTGTGTGCCACCATGCCTGGATAATTTTTGTATTTTTAGTAGAC
AGGGGATTTCACCATGTTGGCCAGGCTGGTCTCAAGCTCCTGACCTCAGGTGA
TCTGCCTGCCTTGGCCTCCCAAAGTGCTGGGATTACAGGCGTGAGCCACCGC
CCCAGCACCCCATTAAATCTTATCACAAAGCCTCTTCAAACTTGGCTCCAATGG
AGGGAATTGATACTTCAGCAATATTCTGTCTTCTACTCCATGAGCATAAACTGA
TGCTATCCTGAGCAAACTAGAATGATTACCCTATGAAGGTTCAGTAACTATAAT
AGGGGTATTTTTGGCATTAGTTTGAGACCTACAGCCTGTGCCAAAAGTGAACAG
AAGCATCACATTTAAAAGATGTATAAAATATGTCTATATCTATCCATTTGATATGG
CTTGACTGTGTCACCACCCAAATCTTATTTGGAATTCCCACATGTTGTAGGAGG
AACCGGTAGGAGGTAATTGAATCATGGGGGCAAGTCTCCCGTGCTATTTTCATG
ATAGTGAATAAGTCTCACGATATCTGATGGTTTTAAAAAAAGGAGTT
RP11-147L13.8 3'RACE
1000bp
500bp
CCCTATCTCTAACCCCCTGCCATGTAGAGAATTGAACTAGCCTTCGCTCTCATA
AGTGGAATTTTAAAAAATAATGAGTTACATGAGCTGATAAGCACACATGCATAG
TCAATGTTAAGGCTTAGCATTTATAAAATTTGGGATGATAATTTATGGCAAATGT
TTAACACATTTAATAAGATAAATAGTTTTTAAGGCATTGAATAGGTAGGAGTTCA
TATGAGTTTACTCTGGGTTGCTATTACTTTTACATAGTCAAACTTTATTTTGTAGT
ATTTTTCTTCTTGATTCTCTAGTCACTATGATAATTATTAGTATGGATGGTGACTT
TTATTTCCAAGCACAGCATAATCCACAATAACATAACATTTAAAAGCAAAGGCT
CTGTATCGATTATTAACATGAACAATTTCCTTTGCTACCATACTCCATCCAGATA
AAGAACTGAATGTTCCTCTGAACCTTCCAATTAATTTCCTCCATTGTGATGAATC
CTCCATAGATTTATTGGCAAAACATTATTTCTAAGTGTTCTCCACCCTACTATAA
ATTGTCTCAAAATAGTTTGTGTCTACCAACAAGGTAGTATAGACTATAAACTTAA
TAAATAGTAATTATTGATAATTATGAGATACCAGGATGCTAATGAAACTTTATTG
CTTGTATTGAGAAATGAGAGTATAAATTGAGTATAAAATGAAAAGACTTGAATG
CTTAGTAAAGCATATAATGTAGCTAAAGTTATTAAACAGATATATGTATATGCC
AAAAAAAAAAAAAAAA

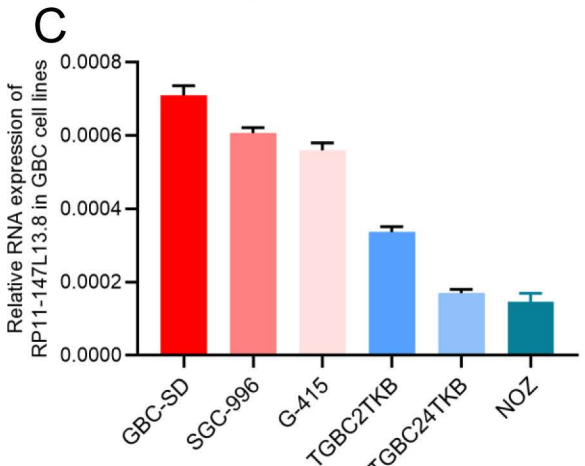
C
Relative RNA expression of RP11-147L13.8 in GBC cell lines
0.0008
0.0006
0.0004
0.0002
0.0000
GBC-SD
SGC-996
G-415
TGBC2TKB
TGBC24TKB
NOZ

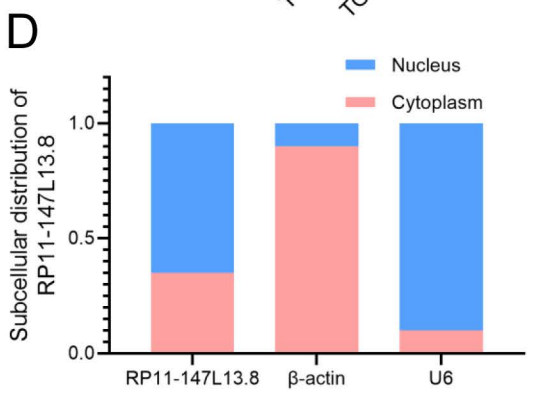
D
Subcellular distribution of RP11-147L13.8
Nucleus
Cytoplasm
1.0
0.5
0.0
RP11-147L13.8
β-actin
U6

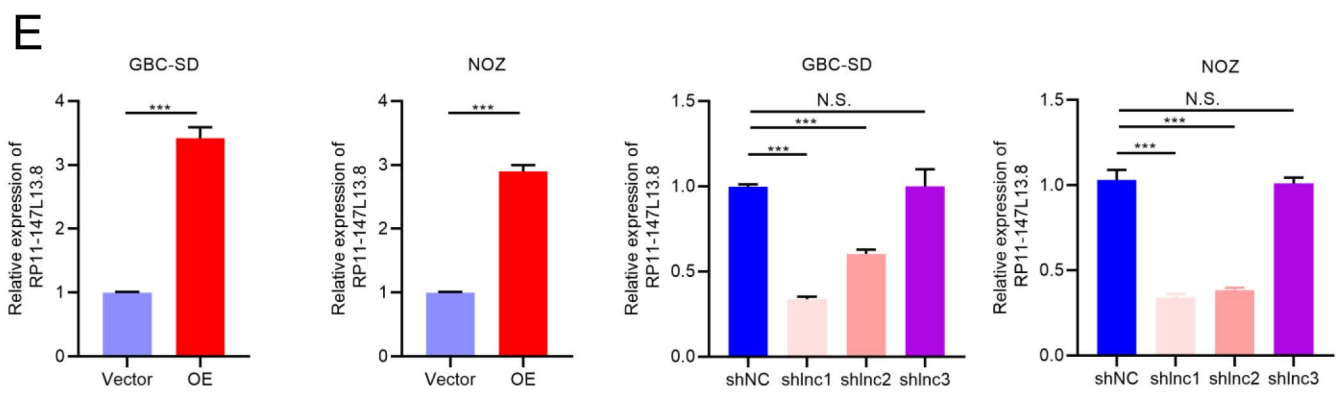
E
GBC-SD
NOZ
GBC-SD
NOZ
Relative expression of RP11-147L13.8
***
N.S.
Vector
OE
shNC
shlnc1
shlnc2
shlnc3

Figure S4

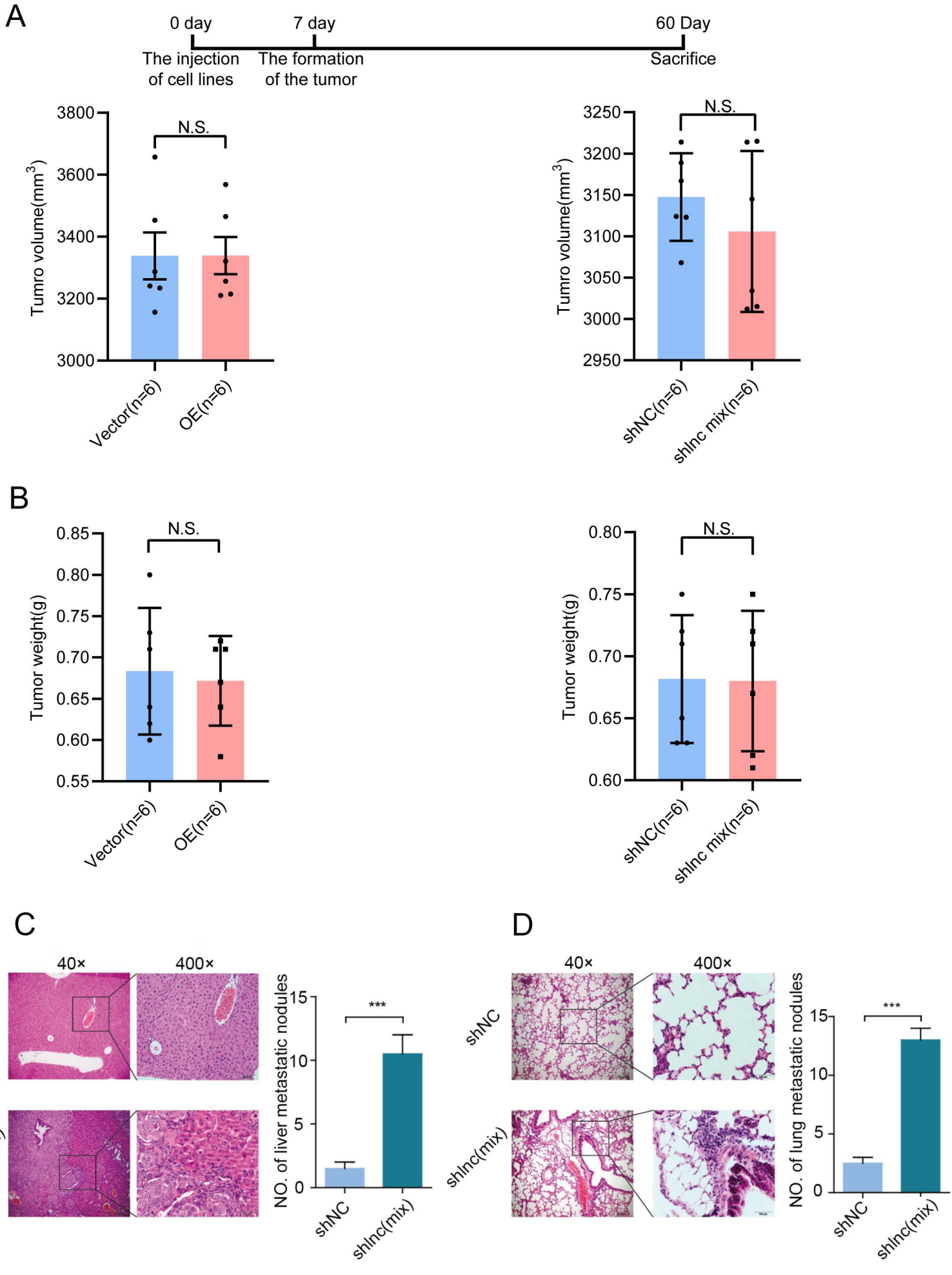
A
0 day
7 day
60 Day
The injection of cell lines
The formation of the tumor
Sacrifice
Tumro volume(mm3)
N.S.
Vector(n=6)
OE(n=6)
shNC(n=6)
shlnc mix(n=6)
B
Tumor weight(g)
C
40×
400×
shNC
shlnc(mix)
NO. of liver metastatic nodules
***
D
NO. of lung metastatic nodules

Figure S5

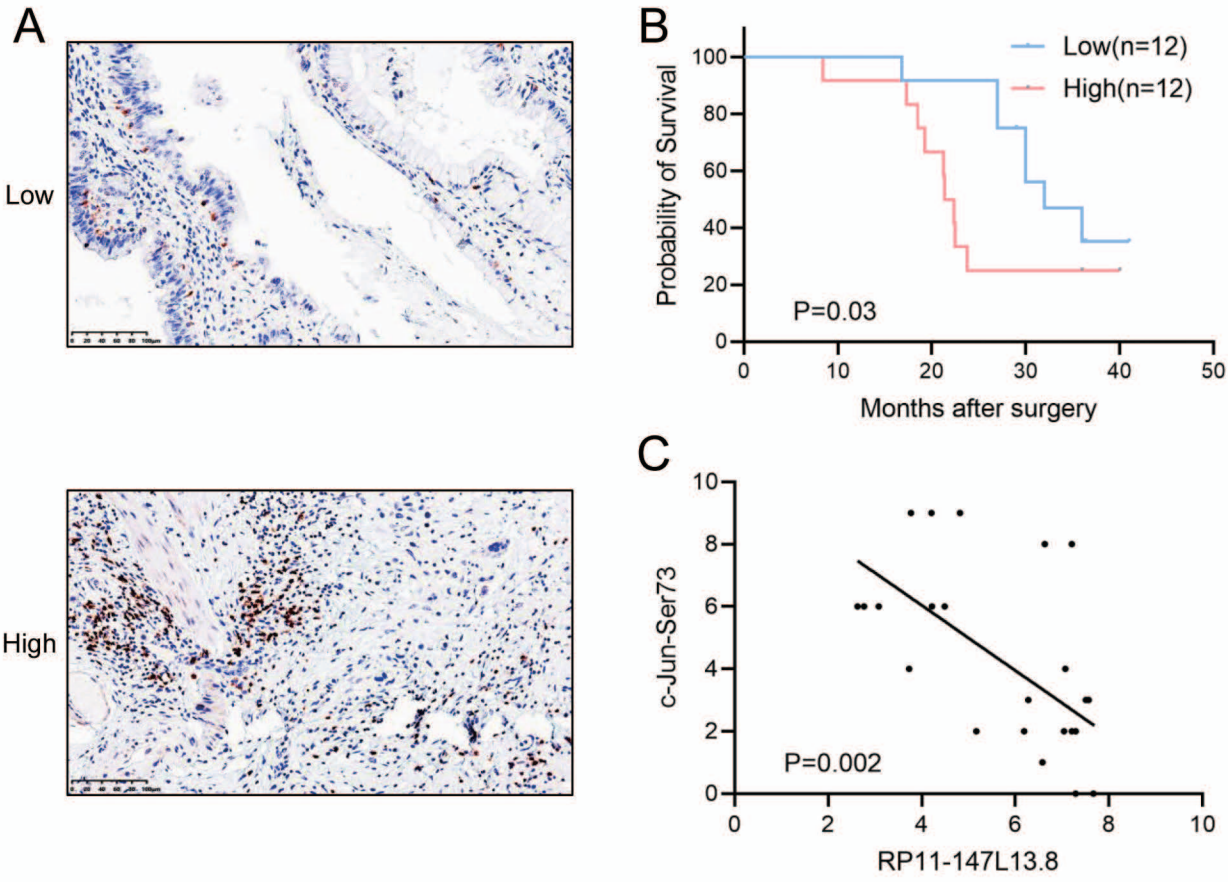
A
Low
High
B
Low(n=12)
High(n=12)
Probability of Survival
100
80
60
40
20
0
P=0.03
0
10
20
30
40
50
Months after surgery
C
c-Jun-Ser73
10
8
6
4
2
0
P=0.002
0
2
4
6
8
10
RP11-147L13.8

Figure S6

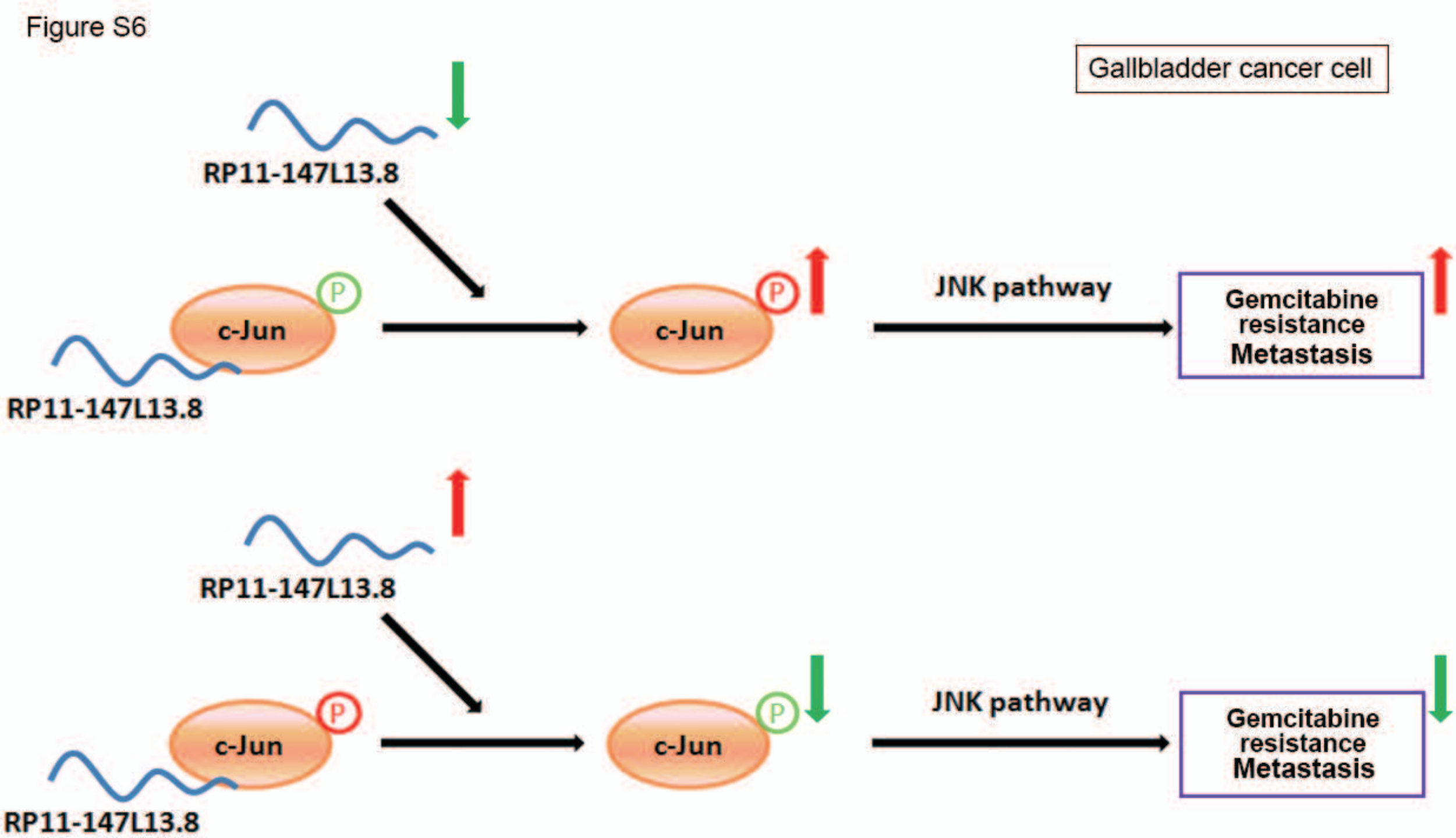
Gallbladder cancer cell
RP11-147L13.8
c-Jun
P
RP11-147L13.8
c-Jun
P
JNK pathway
Gemcitabine resistance Metastasis
RP11-147L13.8
c-Jun
P
RP11-147L13.8
c-Jun
P
JNK pathway
Gemcitabine resistance Metastasis

Table S1 Primers used for reverse transcription-quantitative polymerase chain reaction.

	Forward primer (5’-3’)	Reverse primer (5’-3’)
GAPDH	5’- AGCCACATCGCTCAGACAC-3’	5’- GAATTTGCCATGGGTGGA-3’
RP11-147L13.8	5’- CGATCCTCCCCTCCAACACT-3’	5’-ACTCCAAGGAAGGAACCCCC-3’
LINC01184	5’-AAAGAAGCTGAAAGGGCTCGG-3’	5’-AGCCATCCTCCACTGCAAAC-3’
AC015712	5’-CTGTGGTTCTGCCTCACAGG-3’	5’-TGCCAGATGAGGTTGAGCTG-3’
AC009242	5’-AGACCACCACCACCAATTCC-3’	5’-TGGAGGATGTGCCAGAGGTA-3’
LINC00667	5’-CCGCAGCTGACACCATGAAT-3’	5’-ACCCACCTCTATCTGACGGC-3’
ADAMTS9-AS2	5’-GAGACACAGCTGGGCTGAAC-3’	5’-GCTGCTAGCTCTTCTGGTGC-3’
AC234582	5’-AAAGAAGCTGAAAGGGCTCGG-3’	5’-AGCCATCCTCCACTGCAAAC-3’
LNCTAM34A	5’-AGCGGCATCTCCTCCACCTGAAA-3’	5’-TTGCCTCGTGAGTCCAAGGAGAAT-3’
RNF216P1	5’-AGTGTGGCTGGTATCGGTGT-3’	5’-TGGAGTCACAGGCAGTCGTA-3’
MIR205HG	5’- GGAGTGCAGTGGCTCAATCT-3’	5’- TGGATTGCTTAAGCTCAGGA -3’

Table S2 Primary antibodies used for western blot

Antibodies	Concentration	Specificity	Company	
GAPDH	1:1000 WB	Rabbit mAb	Abcam	EPR13796
c-Jun	1:1000 WB	Rabbit mAb	Cell Signaling Technology	60A8
Phospho-c-Jun (Ser73)	1:1000 WB 1:100 immunohistochemistry	Rabbit mAb	Cell Signaling Technology	D47G9

Table S3 The pull down protein list of the RP11-147L13.8

Accession	Gene Symbol	Description	Coverage [%]	# Peptides	# PSMs	# Unique Peptides
P60709	ACTB	Actin, cytoplasmic 1 OS Homo sapiens GN=ACTB PE=1 SV=1	12	9	8	4
Q86U42	PABP2	Polyadenylate-binding protein 2 OS Homo sapiens GN=PABP2 PE=1 SV=2	30	11	12	5
O95361	TRIM16	Tripartite motif-containing protein 16 OS Homo sapiens GN=TRIM16 PE=1 SV=2	27	6	6	5
Q9NRW3	APOBEC3C	DNA dC->dU-editing enzyme APOBEC-3C OS Homo sapiens GN=APOBEC3C PE=1 SV=2	18	5	5	5
P05412	JUN	Transcription factor AP-1 OS Homo sapiens GN=JUN PE=1 SV=1	35	15	15	14
P67809	YBOX1	Y-box-binding protein 1 OS Homo sapiens GN=YBOX1 PE=1 SV=1	11	7	5	3
E7EX29	E7EX29	14-3-3 protein zeta/delta OS Homo sapiens GN=E7EX29 PE=1 SV=1	9	3	2	1
Q9BQ67	GRWD1	Glutamate-rich WD repeat-containing protein 1 OS Homo sapiens GN=PGRWD1 PE=1 SV=2	10	1	1	1
O43395	PRPF3	U4/U6 small nuclear ribonucleoprotein Prp3 OS Homo sapiens GN=PRPF3 PE=1 SV=2	13	1	1	1

Supplementary Method

RNA sequencing

Total RNAs were collected by TRIzol reagent (Invitrogen), then rRNAs were removed by using the RiboMinus Eukaryote kit (Qiagen, Valencia, CA, USA). We next prepared the RNA-seq libraries using NEBNext Ultra Directional RNA Library Prep Kit (New England Biolabs, Beverly, MA, USA) according to the manufacturer's instructions. The ribosome-depleted RNA libraries were subjected to Illumina HiSeq3000 (Illumina, San Diego, CA, USA) for sequencing. The raw sequencing reads were first processed to clip adapter sequences and low-quality bases by software Trimmomatic. Afterward, all filtered reads were aligned to the human reference genome (hg38) using the splice-aware aligner HISAT2. The Cufflinks program was used to calculate the gene expression level in FPKM units (FPKM = Fragments Per Kilobase of transcript per Million mapped reads).

Survival analysis

Survival analysis was performed as described in a previous study [39]. Details were listed in the supplementary materials. Briefly, the expression levels of each lncRNA across all tumor samples in each sample group were used to explore whether they were associated with the prognosis status of tumor patients. For each lncRNA, GBC tumor samples were divided into two groups according to the median value of the expression. Then, the log-rank test was used to compare the difference between the two groups.

Northern blot assays and western blot assays

The Ambion Northern Max-Gly Kit (Austin, Texas, USA) was employed to detect *RP11-147L13.8* RNA levels in tissue and cells. Briefly, the nylon membrane (NC) with a positive charge was utilized to electrophorese and siphon the extracted total RNA samples. UV cross-linking was conducted to fix the RNA on the NC membrane. Then, the DIG Northern Starter Kit (Roche, Indianapolis, Indiana, USA) with a Digoxin-labelled RP11-147L13.8-specific oligonucleotide probe was employed to detect *RP11-147L13.8*.

The SDS-PAGE was employed to separate proteins and transfer proteins to nitrocellulose membranes (Bio-Rad, Hercules, California, USA), which were blocked with 5% non-fat milk and incubated with corresponding primary antibodies followed by horseradish peroxidase-conjugated secondary antibodies. Then, the chemiluminescence ECL reagents (Pierce Biotechnology, Illinois, USA) were utilized for visualization of the immunoreactivity. Additionally, the densitometry was measured by Image-Pro Plus 6.0 (Media Cybernetics, Maryland, USA).The antibody used for western blot assays were listed is **Table S2**.

RNA interference and lentivirus construction

The short hairpin RNA (shRNAs) oligonucleotides used for RP11-147L13.8 in the current study were purchased from RiboBio (Guangzhou, China). The human RP11-147L13.8 sequence was amplified from cDNAs. The pCDH-RP11-147L13.8 was generated by cloning the RP11-147L13.8 sequence into the BamHI and EcoRI sites of pCDH lentiviral vectors. The pCDH, pCDH-RP11-147L13.8 were transfected along with the packaging plasmid psPAX2 and the envelope plasmid pMD2G into the GBC cell lines by using Lipofectamine 2000 (Invitrogen) according to the manufacturer's instructions. The virus particles were collected 48h after transfection then were infected into GBC cells with recombinant lentivirus-transducing units using 1 μg/ml polybrene (Sigma-Aldrich, Missouri, USA).

***In vitro* cell migration and invasion assays and *in vivo* metastasis assays**

The invasion assays were performed in Millicell chambers that were coated with 30μg of Matrigel (BD Biosciences, Franklin Lakes, New Jersey, USA). Similar operations were conducted in the migration assays but without a coated membrane. The cells (5×10^4 and 1×10^5 for migration and invasion assays, respectively) were added to the upper chambers. DMEM containing 10% FBS was placed into the lower chambers as a chemoattractant. The cells were then incubated at 37℃ with 5% CO_2 for 24h. After the incubation, we fixed the cells that migrated or invaded through the filters with 20% methanol. Then fixed cells were then stained with 0.1% crystal violet. We randomly selected five fields to count the cell numbers by using an inverted microscope (Olympus, Tokyo, Japan).

Nude mice (female BALB/c-nu/nu mice) were purchased from the Experimental Animal Center of Shanghai Cancer Institute (Shanghai, China) for our *in vivo* metastasis assays. GBC-SD cells (1×10^6 sh vector or stable sh*RP11-147L13.8* GBC-SD cells) that were suspended in 0.2 ml serum-free DMEM were injected subcutaneously into each mouse (10 mice for each group) through the right axilla. The tumor growth was monitored. The mice were sacrificed after 60 days, then livers and lungs were dissected. The liver and lung tissue derived from the mice were fixed with phosphate-buffered neutral formalin and prepared for the following histological examination. The hematoxylin-eosin (H&E) staining was utilized to determine the number of metastatic foci in the liver or lung tissue under a binocular microscope (Leica, Wetzlar Lottehaus, Germany). The tumor volume was measured as length × width^2 × 0.5. Experiments performed in this part were all under the regulations of the Shanghai Medical Experimental Animal Care Commission.

RNA pull-down assays, mass spectrometry analyses, and RNA immunoprecipitation (RIP) assays

First, *RP11-147L13.8* and antisense *RP11-147L13.8* were transcribed *in vitro* and labeled with the Biotin RNA Labelling Mix (Roche, USA). The RNA samples were treated with RNase-free DNase I (Takara, Japan) then purified with an RNeasy Mini Kit (QIAGEN, USA). Second, to format an appropriate secondary structure, an RNA structure buffer was used to pre-treat the biotinylated RNAs. Then the pre-treated biotinylated RNAs were incubated with 1 mg protein extracts at 4℃ for 1 h. After the incubation, 40 μl streptavidin-linked magnetic beads (ThermoFisher, USA) were utilized to perform the pull-down at room temperature for 2h. Next, the beads-RNA-proteins mixture was washed in 1 × washing buffer (5mM Tris-HCl, 1 M NaCl, 0.5 mM EDTA, and 0.005% Tween 20) five times. The precipitation and dilution were conducted in 60 μl protein lysis buffer, then the proteins were separated by using gel electrophoresis. And the visualization was shown after silver staining according to the manufacturer's instructions. Finally, the retrieved proteins were measured on SDS-PAGE gels for mass spectrometry analysis (Shanghai Applied Protein Technology, Shanghai, China) or Western blot.

The Magna RIP RNA-binding protein immunoprecipitation kit (Millipore, Massachusetts, USA) was employed to conduct the RIP assays in the current study. In brief, lysis buffer (0.5 ml) were utilized to lyse cells in 10 cm dishes with protease inhibitors and RNase Inhibitor (Thermo Fisher Scientific, Illinois, USA) according to the manufacturer's instructions. The lysed cells were then subjected to centrifuge at 12,000 r.p.m. for 30 min. Then the supernatants were incubated with Protein G Dynabeads (Thermo Fisher Scientific, California, USA) and indicated antibodies. After incubation at 4℃ for 12 h, the beads were washed thrice with wash buffer then twice with PBS. Both the wash buffer and PBS contained RNase inhibitor. The Total RNA isolation kit (Thermo Fisher Scientific) was employed to extract co-precipitated RNAs, which were then subjected to qRT-PCR assays.

Immunoblotting analysis and co-immunoprecipitation (Co-IP).

The immunoblotting analysis was The lysis buffer (Beyotime Biotechnology, Shanghai, China) with protease inhibitors (Roche, Indiana, USA) was employed to lyse cells (5×10^6). The BCA method was used to determine protein concentrations (Pierce, Thermo Fisher Scientific, Illinois, USA). SDS-PAGE was utilized to analyze the samples after centrifugation at 4℃ for 15 min. The samples then were transferred to PVDF membranes (Immobilon-P membrane, Millipore, Massachusetts, USA) and HRP-conjugated secondary antibodies were employed in the following immune blotting analysis. Specifically, TBS plus Tween 20 with skimmed milk (5%) were used to block the membranes at 4℃ before the probing was conducted. Finally, the assay results were visualized by employing the Enhanced Chemiluminescence Plus Westen Blotting Detection Systems (GE Healthcare, Connecticut, USA) and LAS-4000EPUV mini Luminescent Image Analyzer with enhanced chemiluminescent (ECL) chromogenic substrates.

The details of the Co-IP were listed below. Briefly, plasmids were transiently transfected to cell lines at the 60% confluence for 48 h, and then cells in a 10 cm dish were lysed by 0.3% NP40 (with protease inhibitor, 1 mM PMSF, and phosphatase inhibitor, 1 mM Na_3VO_4) on ice. Cell lysates were incubated with GFP, Flag, or HA

beads overnight at 4 °C. Protein precipitate was harvested through centrifugation at 12,000 rpm for 10 min, washed with PBS, added with 2 × SDS sample buffer for immunoblotting samples preparation. Protein samples were separated by SDS-PAGE electrophoresis, transferred onto PVDF membrane, blocked with 5% non-fat milk for 1 h at room temperature, incubated with primary antibody overnight at 4°C, washed with PBST three times for 10 min each time, then incubated with HRP-conjugated secondary antibody for 1h at room temperature, and washed with PBST three times for 10 min each time. Finally, the target proteins were visualized.

5′ and 3′ rapid amplification of cDNA ends (RACE) analysis

Total RNA was isolated using TRIzol Plus RNA Purification Kit (Invitrogen), according to the manufacturer's instructions. 5′ RACE and 3′ RACE were performed using GeneRacer™ Kit (Invitrogen) according to the manufacturer's instructions. The following gene-specific primers (GSP) are used for PCR: 5′-ATCGATTAAGGAGGAATAAAGTCAACC-3′ (5′ RACE GSP1), 5′-CCCGACAGTCACTCGAACCAGTCGAACC-3′ (5′ RACE GSP2), 5′-CCAGGTTTTGATCTCCTTGAAGCTCCACCTC-3′ (3′ RACE GSP1), 5′-CACCCGCTATATTGGCGCCACTGTAC-3′ (3′ RACE GSP2).

The isolation of cytoplasmic and nuclear RNA

According to the manufacturer's instructions Cytoplasmic and nuclear RNAs of NOZ cells were extracted and purified using PARIS™ Kit (Invitrogen).

The establishment of gemcitabine-resistant GBC-SD cell line

The GBC cell line, GBC-SD, was cultured in DMEM (Sigma–Aldrich-Merk, Darmstadt, Germany) complete medium containing 10% fetal bovine serum (FBS) (Sigma–Aldrich-Merk, Darmstadt, Germany), 100 U/mL penicillin, and 100 μg/mL streptomycin (Life Technologies Gathersburg, MD, USA). The gemcitabine resistant

clone, named GBC-R, was obtained by exposing parental cells intermittently to escalating doses of the drug, starting from 10 nM of GEM to 1.5 μM for 9 months. After another 3 months of being continuously cultured in the presence of 1.5 μM, the GBC-R1.5 cells were considered stable.